X-321-71-174
PREPRINT

NASA TM X-65617

THE NASTRAN HYDROELASTIC ANALYZER

JAMES B. MASON

MARCH 1971

GSFC
GODDARD SPACE FLIGHT CENTER
GREENBELT, MARYLAND

X-321-71-174

THE NASTRAN HYDROELASTIC ANALYZER

James B. Mason
Test and Evaluation Division
Systems Reliability Directorate

March 1971

GODDARD SPACE FLIGHT CENTER
GREENBELT, MARYLAND

THE NASTRAN HYDROELASTIC ANALYZER

Prepared by: James B. Mason

James B. Mason
Structural Dynamics Branch

Reviewed by: W. R. Forlifer

William R. Forlifer
Assistant Head, Structural Dynamics Branch

Edward J. Kirchman

Edward J. Kirchman
Head, Structural Dynamics Branch

Approved by: F. Starbuck for

John C. New
Chief, Test and Evaluation Division

REPORT STATUS

This report describes the general capabilities, limitations, and characteristics of the NASTRAN Hydroelastic Analyzer.

AUTHORIZATION

Test and Evaluation Division Charge Number 321-124-08-12-01

THE NASTRAN HYDROELASTIC ANALYZER

James B. Mason
Test and Evaluation Division

SUMMARY

An overview of the NASTRAN Hydroelastic Analyzer computer program is given. Included is a theoretical derivation showing general assumptions and procedures used in obtaining the finite element model of the hydroelastic problem. Program implementation of the theory is discussed, and an Appendix showing a comparison between NASTRAN and theoretical results is attached.

THE NASTRAN HYDROELASTIC ANALYZER

The motions of liquids and gases in various containers has been of interest for many years.* One particular area where these effects are of great importance is in the analysis and design of missile and space vehicle structures. In these type structures, where lightweight-thin-walled construction is typical, the containers cannot be considered rigid and coupling of the various fluid motions with the elastic deformations of the tank must be considered. This so-called hydroelastic problem and, in particular, its solution using the NASTRAN computer program is the subject of this report.

The NASTRAN (NASA STRUCTURAL ANALYSIS) computer program is a general purpose finite element program developed for the analysis of large and/or complex structures. It was decided that the addition of certain fluid capability to this program would result in a useful hydroelastic analyzer for the solution of many important problems. Other advantages arising from this approach would be that many automated features already existing in NASTRAN would apply to the resulting hydroelastic analyzer. For example, since the existing structural program had the capability of treating control systems, the resulting hydroelastic analyzer could include the coupled interactions of the fluid, the structure, and the control system for problems where these influences are of concern.

The addition of the hydroelastic capability was accomplished by the MacNeal-Schwendler Corporation under contract to the Goddard Space Flight Center. This capability is presently operational on the IBM 360-95 computer.

It is the purpose of this report to present the general capabilities, limitations, and characteristics of this new hydroelastic analyzer. To accomplish this, a theoretical derivation is given first which presents general assumptions and procedures used in obtaining a finite element statement of the hydroelastic problem. The derivation is not limited by topology considerations and discretization is symbolically indicated with no associated finite element property specification.

The program implementation of the theory is then discussed. Topological limitations and fluid element properties employed in the program are given. General input/output data and user selected solution requests are reviewed. The report concludes with a summary of the capabilities and limitations associated with the hydroelastic analyzer.

* For example, see Abramson, H. N., "The Dynamic Behavior of Liquids in Moving Containers," NASA SP-106.

An Appendix is included showing a comparison of NASTRAN and theoretical results for several sample problems. Gases and liquids with free surfaces are treated here, and eigenvalue and forced response solutions are obtained.

The basis for the analytical developments reported herein is the work by the MacNeal Schwendler Corporation and, in particular, the derivations by Dr. R. H. MacNeal and D. N. Herting, see references (1) and (2). The theoretical developments in this report, however, present an alternative formulation of many aspects of the hydroelastic problem. It is hoped that this reformulation will provide the prospective user with both an overfiew of the program and a document which can serve as an aid when used in conjunction with the above references.

THEORETICAL DEVELOPMENT

The problem to be treated is that of a compressible fluid in an elastic container. Only small motions from the undistrubed state of the coupled fluid-structure system are considered. We desire the pressure to be the basic unknown of the fluid and the deformation to be the basic unknown for the structure.

In this section, the governing differential equations describing the pressure distribution in the fluid continium are derived. A variational statement equivalent to these governing equations and boundary conditions is then obtained. From this variational statement, the matrix equations of the finite element fluid model are indicated. The final set of finite element matrix equations describing the hydroelastic problem are then obtained by combining the equations describing the fluid and structural systems.

Fluid Description – Differential Equations

We assume that the mass density ρ_d of the disturbed fluid never varies greatly from its undisturbed value ρ . Thus, we may write

$$\rho_d = \rho\,(1 + s) \tag{1}$$

where $s = s\,(x, y, z, t)$ is the condensation and is small compared to unity.

We also assume that disturbances propagate through the fluid by an adiabatic process. With this assumption, we relate the pressure p to the density by the state equation

$$p = p\,(\rho_d) \tag{2}$$

Expanding (2) about the undisturbed condition and using (1), we obtain

$$p = p_0 + \frac{\partial p}{\partial \rho_d} \cdot s\,\rho + \cdots \text{ higher order terms} \tag{3}$$

where p_0 is the undisturbed pressure. For an adiabatic process

$$p = \frac{p_0}{\rho^\gamma}\,\rho_d^\gamma \tag{4}$$

where γ is the ratio of specific heats at constant pressure to constant volume. Substituting (4) into (3) and using (1) yields

$$\begin{aligned} p &= p_0 + \frac{p_0}{\rho^\gamma}\,\gamma\,\rho_d^{(\gamma-1)} \cdot s\,\rho = p_0 + a_0^2 \cdot s\,\rho = p_0 + a_0^2 \cdot (\rho_d - \rho) \\ &= \text{constant} + a_0^2\,\rho_d \end{aligned} \tag{5}$$

In the above, the speed of sound a_0 through the undisturbed fluid has been used since

$$\gamma \cdot \frac{p_0}{\rho^\gamma}\,\rho_d^{(\gamma-1)} \doteq \gamma \cdot \frac{p_0}{\rho} \cdot [1 + (\gamma - 1)\,s] \doteq \gamma\frac{p_0}{\rho} = a_0^2 \tag{6}$$

Neglecting nonlinear and viscous terms in the equations of motion and assuming that the fluid velocities are small compared with a_0, Euler's equations take the form*

---

* Note that $\frac{\partial ()}{\partial t} = (\dot{\ })$

$$\rho_d \ddot{\vec{u}} = - \vec{\nabla} p - \rho_d \vec{g} \tag{7}$$

where $\vec{u}$ is a small displacement of the fluid from a fixed reference point and only gravitational body forces $\rho_d \vec{g}$ are assumed acting. Substituting (1) into (7) and neglecting products of small terms, results in the equations of motion

$$\rho \ddot{\vec{u}} = - \vec{\nabla} p - \rho \vec{g} \tag{8}$$

The continuity equation can be expressed as

$$\dot{\rho}_d + \vec{\nabla} \cdot \rho_d \dot{\vec{u}} = 0 \tag{9}$$

Using (5), equation (9) may be written as

$$\frac{1}{a_0^2} \dot{p} + \vec{\nabla} \cdot \rho_d \dot{\vec{u}} = 0 \tag{10}$$

Substituting (1) into (10) and neglecting products of small terms results in the equation of continuity in the form

$$\frac{1}{a_0^2} \dot{p} + \rho \vec{\nabla} \cdot \dot{\vec{u}} = 0 \tag{11}$$

The particle velocity $\dot{\vec{u}}$ may be eliminated from (8) and (11) by taking the first time derivative of (11) and the divergence of (8), then the three dimensional wave equation

$$\frac{1}{\rho a_0^2} \ddot{p} = \vec{\nabla} \cdot \frac{1}{\rho} \vec{\nabla} p + \vec{\nabla} \cdot \vec{g} \tag{12}$$

in terms of pressure is obtained. The quantity $\rho_0 a_0^2$ is equal to the adiabatic bulk modulus B of the fluid. Thus, equation (12) can be written in the form

$$\frac{1}{B}\ddot{p} - \vec{\nabla}\cdot\frac{1}{\rho}\vec{\nabla}p = \vec{\nabla}\cdot\vec{g} \tag{13}$$

In the following developments the effects of the gravity gradient are neglected and the wave equation takes the final form

$$\frac{1}{B}\ddot{p} - \vec{\nabla}\cdot\frac{1}{\rho}\vec{\nabla}p = 0 \tag{14}$$

The boundary conditions to be considered are of two types:

$$p = \text{prescribed on boundary surfaces } S_2 \tag{15a}$$

$$\frac{1}{\rho}\frac{\partial p}{\partial n} = -q_n \text{ on boundary surface } S_1 \tag{15b}$$

Here $\partial p/\partial n$ is the derivative of p in the direction of the outer unit normal $\hat{n}$ to the boundary surface and q_n is a generalized normal flux per unit surface area. It will be shown subsequently that condition (15a) corresponds to fluid free surface points in the absence of a gravity field while (15b) corresponds to the conditions at both a free surface when gravity is present and points on a fluid-structure boundary.

Fluid Description – Finite Element

While the variational statement of a problem is not required for the application of the finite element method, this approach does provide a clarity and consistency to the finite element formulation and is adopted here.

From the results of variational calculus, see references (3) and (4), it is known that for the functional*

$$H(p) = \underbrace{\int_V \left\{ \frac{1}{B} \ddot{p}\, p + \frac{1}{2\rho} \vec{\nabla} p \cdot \vec{\nabla} p \right\} dV}_{\text{(volume)}} + \underbrace{\int_{S_1} q_n\, p\, dS}_{\text{(surface)}} \tag{16}$$

to attain a minimum, then the pressure must satisfy the Euler equation (14) through the volume and the conditions (15) on the boundary. Thus, equation (16) can be viewed as an alternative statement of the fluid problem. Taking the variation of (16) and considering $\ddot{p}$ as an invariant, we have

$$\delta H(p) = \int_V \left\{ \frac{1}{B} \ddot{p}\, \delta p + \delta \left(\frac{1}{2\rho} \vec{\nabla} p \cdot \vec{\nabla} p \right) \right\} dV + \int_{S_1} q_n\, \delta p\, dS = 0 \tag{17}$$

so that

$$\int_V \frac{1}{B} \ddot{p}\, \delta p\, dV + \int_V \frac{1}{\rho} \vec{\nabla} p \cdot \delta \vec{\nabla} p\, dV = - \int_{S_1} q_n\, \delta p\, dS \tag{18}$$

represents the variational statement of the problem for the continuous fluid system. We note here the similarity of (18) with the principle of virtual work for dynamic loading in a continuous structural system. From this viewpoint, the first term on the left of (18) can be associated with the virtual work of "generalized inertia forces" $(1/B)\ddot{p}$, the second term with the "generalized strain energy" of the fluid volume, and the right hand side of the equation with the virtual work of "distributed generalized surface forces" q_n.

The discretization of the fluid system in terms of a finite number of degrees of freedom p_j is obtained from the variational statement (18) using standard procedures (see references (3) and (5)). To acomplish this, we relate the pressure p in the continuous system to the degrees of freedom $p_j = \{p_1\ p_2 \cdots\}$ by the matrix equation

* Note that $\ddot{p}$ is considered invariant and p is not constrained on S_1.

$$p = [a]\ \{p_j\} \tag{19}$$

where $[a]$ is a function of position. Similarly, the pressure gradient may be related to $\{p_j\}$ by the matrix expression*

$$\vec{\nabla} p = \{\nabla p\} = [b]\ \{p_j\} \tag{20}$$

From (19) and (20), we obtain the virtual quantities

$$\delta p = [a] \cdot \{\delta p_j\} \tag{21a}$$

$$\delta \vec{\nabla} p = \delta \{\nabla p\} = [b] \cdot \{\delta p_j\} \tag{21b}$$

Substituting (19) through (21) into (18) and noting that the virtual pressures are arbitrary, results in the matrix equations of motion

$$[M^F] \cdot \{\ddot{p}_j\} + [K^F] \cdot \{p_j\} = \{I_j\} \tag{22}$$

for the idealized fluid system. In (22) we have

$$[M^F] = \int_V [a]^T \frac{1}{B} [a] \cdot dV \tag{23}$$

* Note that the form of $[a]$ and $[b]$ is determined by the character of the spatial pressure distribution assumed for the finite fluid elements. Here we symbolically represent these matrices and defer discussion of the fluid element properties until the next section.

$$[K^F] = \int_V [b]^T \frac{1}{\rho} [b] \, dV \tag{24}$$

$$\{I_j\} = - \int_{S_1} [a]^T q_n \, dS \tag{25}$$

where the superscript F refers to the fluid. Examination of (23) and (24) shows that the "generalized fluid mass matrix" $[M^F]$ includes fluid compressibility effects while fluid mass effects are included in the "generalized fluid stiffness matrix" $[K^F]$.

The vector $\{I_j\}$ represents "concentrated generalized surface forces" due to the distributed generalized surface forces q_n. We observe that the forces I_j do work through their conjugate generalized degrees of freedom p_j and that I_j is nonzero only on those degrees of freedom associated with the S_1 boundary where q_n is defined.

Two general types of boundary conditions are considered in the hydroelastic problem; they are:

(1) Fluid-structure boundary
(2) Fluid free surface boundary

where the second condition is associated with gravity wave effects of liquids in containers. With these considerations, it is convenient to reorder and partition (22) into the form

$$\left[\begin{array}{c:c:c} M^F_{ii} & M^F_{if} & M^F_{is} \\ \hdashline M^F_{if} & M^F_{ff} & M^F_{fs} \\ \hdashline M^F_{is} & M^F_{fs} & M^F_{ss} \end{array}\right] \left\{\begin{array}{c} \ddot{p}_i \\ \hdashline \ddot{p}_f \\ \hdashline \ddot{p}_s \end{array}\right\} + \left[\begin{array}{c:c:c} K^F_{ii} & K^F_{if} & K^F_{is} \\ \hdashline K^F_{if} & K^F_{ff} & K^F_{fs} \\ \hdashline K^F_{is} & K^F_{fs} & K^F_{ss} \end{array}\right] \left\{\begin{array}{c} p_i \\ \hdashline p_f \\ \hdashline p_s \end{array}\right\} = \left\{\begin{array}{c} 0 \\ \hdashline I_f \\ \hdashline I_s \end{array}\right\} \tag{26}$$

where the subscripts in the above are fluid degree of freedom identifications defined as

i = degrees of freedom associated with the fluid interior
f = degrees of freedom associated with the fluid free surface boundary
s = degrees of freedom associated with the fluid-structure boundary

Expressions for the concentrated generalized surface forces I_s and I_f applied, respectively, to the fluid-structure and free surface degrees of freedom will now be obtained. Examination of (25) shows that this requires knowledge of the generalized surface force (or flux) at these boundaries.

At a fluid-structure boundary, no fluid may penetrate the structural boundary and no gaps may occur between the fluid and the structure. For the nonviscous fluid considered, this means that the fluid acceleration component normal to the boundary must equal the acceleration of the structural boundary normal to itself. From (8) and the acceleration compatibility condition, we may write

$$\frac{1}{\rho} \frac{\partial p}{\partial n} = - \ddot{u}_n^s - \vec{g} \cdot \hat{n} \tag{27}$$

at the boundary. In the above:

$$\frac{1}{\rho} \frac{\partial p}{\partial n} = \frac{1}{\rho} \vec{\nabla} p \cdot \hat{n}$$

$\hat{n}$ ≡ outward unit normal at the fluid-structure boundary

$\ddot{u}_n^s$ ≡ normal component of the structural acceleration at the fluid-structure boundary

Comparing (27) with (15b) we see that the generalized normal flux at the fluid-structure boundary is

$$q_n = \ddot{u}_n^s + \vec{g} \cdot \hat{n} \tag{28}$$

Substituting (28) into (25) and neglecting the static gravity effects (since all motions are measured from static equilibrium) results in the expression

$$\{I_s\} = - \int_{S_s} [a_s]^T \ddot{u}_n^s \, dS \tag{29}$$

for the concentrated forces applied to the fluid-structure freedoms p_s. S_s is the fluid-structure boundary area portion of S_1.

The boundary condition problem at a free surface is rather unique. This arises from the fact that while the boundary condition at the free surface is known, i.e.

$$\bar{p} = \text{pressure at the free surface} = 0 \tag{30}$$

since measurement is made from static equilibrium, the location of this boundary is not. The method adopted for the program stems from the Eulerian description used in fluid mechanics where the analysis views a point fixed in space, see sketch below

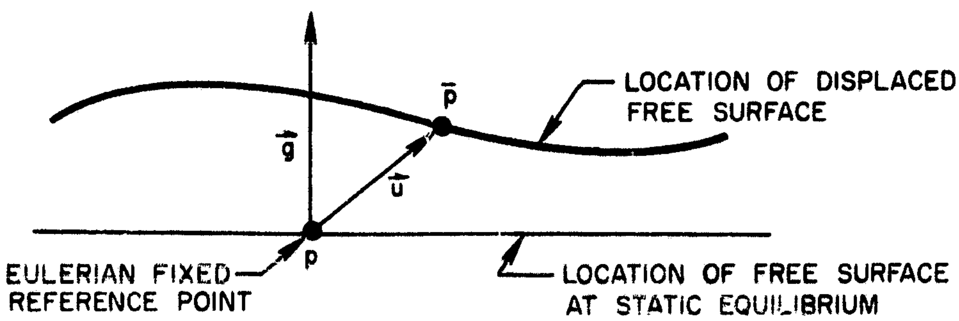

To determine the pressure p at a point in space originally located on the free surface at static equilibrium, we expand in a Taylor's series about $\bar{p}$ on the displaced surface. Thus, we obtain

$$p = \bar{p} - \vec{u} \cdot \vec{\nabla} p + \dots \doteq - \vec{u} \cdot \vec{\nabla} p \tag{31}$$

since $\bar{p} = 0$ and higher order terms have been neglected. Using (8) in (31) and neglecting higher order terms, we obtain

$$p = \rho\, \vec{u} \cdot (\ddot{\vec{u}} + \vec{g}) \div \rho\, \vec{g} \cdot \vec{u} \tag{32}$$

Assuming that $\vec{g}$ is positive in the direction of the outward normal to the original free surface permits (32) to be written in the form

$$p = \rho\, g\, u_n^F \tag{33}$$

where

g ≡ magnitude of the gravity vector

u_n^F ≡ fluid free surface displacement component parallel to the gravity vector.

Differentiating (33) twice with respect to time yields

$$\ddot{p} = \rho\, g\, \ddot{u}_n^F \tag{34}$$

By a procedure like that leading to (28) we may obtain the generalized normal flux at the free surface as

$$q_n = \ddot{u}_n^F + \vec{g} \cdot \hat{n} \tag{35}$$

Substituting (34) into (35) yields

$$q_n = \frac{\ddot{p}}{\rho\, g} + \vec{g} \cdot \hat{n} \tag{36}$$

Substituting (36) into (25) and neglecting static effects results in the expression

$$\{I_f\} = - \int_{S_f} [a_f]^T \frac{\ddot{p}}{\rho\, g}\, d\,S \tag{37}$$

for the concentrated forces applied to the free surface freedoms p_f. S_f is the free surface boundary area portion of S_1.

In the absence of a gravity field we see from (32) that the free surface boundary condition becomes

$$p = 0 \tag{38}$$

Comparing (38) with (15a) and the variational statement of the fluid problem, we see that (38) is an "essential boundary condition" while those represented by (29) and (37) are "natural boundary conditions." Cases represented by (38), where the pressure is prescribed to be zero over an area S_2, are treated automatically in the program by the application of constraints requiring

$$\{p_f\} = \{0\} \tag{39}$$

The results of (29) and (37) are now to be put into a form suitable for use in a general matrix statement of the hydroelastic problem. To accomplish this, the character of the finite fluid elements defining $[a_s]$ and $[a_f]$ must be known and assumptions and numerical procedures for the integrations defined. In addition, for $[I_s]$ the independent degrees of freedom and the type of finite elements used for representation of the idealized structure must be considered. Complete details of the procedure are presented in references (1) and (2).

For the present, it will be satisfactory to assume that the discretization process associated with (29) and (37) has been accomplished. Symbolically indicating this for the concentrated forces applied to the fluid degrees of freedom p_s at the fluid-structure boundary, we write (29) in the form

$$\{I_s\} = - [A]^T \{\ddot{u}^S_{n_s}\} \tag{40}$$

where

$\ddot{u}^{S}_{n_{\bar{s}}}$ ≡ normal structural displacement components of the finite element structural model at structural degrees of freedom on the fluid-structural boundary associated with fluid degrees of freedom p_s*.

$[A]^T$ ≡ rectangular matrix describing the interconnection of the fluid and structure. This matrix reflects the structural degrees of freedom used in the analysis and the structural boundary areas associated with these freedoms.

Similarly, the concentrated forces applied to the fluid degrees of freedom p_f at the free surface can be indicated by writing (37) as

$$\{I_f\} = [M]\{\ddot{p}_f\} \tag{41}$$

where

$\lfloor M \rceil$ ≡ square matrix describing the free surface effects. This matrix includes gravity and fluid density effects.

Equations (40) and (41) may now be included in the general matrix statement of the fluid problem. Noting that (41) has the form of a generalized fluid mass coefficient, we may write (26) in the form

$$\left[\begin{array}{c|c|c} M^F_{ii} & M^F_{if} & M^F_{is} \\ \hline M^F_{if} & M^F_{ff} + M & M^F_{fs} \\ \hline M^F_{is} & M^F_{fs} & M^F_{ss} \end{array}\right] \left\{\begin{array}{c} \ddot{p}_i \\ \hline \ddot{p}_f \\ \hline \ddot{p}_s \end{array}\right\} + \left[\begin{array}{c|c|c} K^F_{ii} & K^F_{if} & K^F_{is} \\ \hline K^F_{if} & K^F_{ff} & K^F_{fs} \\ \hline K^F_{is} & K^F_{fs} & K^F_{ss} \end{array}\right] \left\{\begin{array}{c} p_i \\ \hline p_f \\ \hline p_s \end{array}\right\} = \left\{\begin{array}{c} 0 \\ \hline 0 \\ \hline -[A]^T\{\ddot{u}^S_{n_{\bar{s}}}\} \end{array}\right\} \tag{42}$$

* Note that the subscripts s and $\bar{s}$ refer to fluid and structural degrees of freedom, respectively, on the fluid structure boundary. There is no requirement that $s = \bar{s}$ and, in fact, this will usually not be the case.

Structure Description – Finite Element

The finite element displacement formulation of the structural dynamics problem is well known and is not repeated here, see references (2), (3), and (5) for details. For our purposes, we express the Lagrangian matrix statement of the discretized structural mechanics problem in the partitioned form

$$
\left[\begin{array}{c|c|c}
M^S_{n_{\bar{s}}n_{\bar{s}}} & M^S_{n_{\bar{s}}t_{\bar{s}}} & M^S_{n_{\bar{s}}r} \\ \hline
M^S_{n_{\bar{s}}t_{\bar{s}}} & M^S_{t_{\bar{s}}t_{\bar{s}}} & M^S_{t_{\bar{s}}r} \\ \hline
M^S_{n_{\bar{s}}r} & M^S_{t_{\bar{s}}r} & M^S_{rr}
\end{array}\right]
\left\{\begin{array}{c}
\ddot{u}^S_{n_{\bar{s}}} \\ \hline
\ddot{u}^S_{t_{\bar{s}}} \\ \hline
\ddot{u}_r
\end{array}\right\}
+
\left[\begin{array}{c|c|c}
K^S_{n_{\bar{s}}n_{\bar{s}}} & K^S_{n_{\bar{s}}t_{\bar{s}}} & K^S_{n_{\bar{s}}r} \\ \hline
K^S_{n_{\bar{s}}t_{\bar{s}}} & K^S_{t_{\bar{s}}t_{\bar{s}}} & K^S_{t_{\bar{s}}r} \\ \hline
K^S_{n_{\bar{s}}r} & K^S_{t_{\bar{s}}r} & K^S_{rr}
\end{array}\right]
\left\{\begin{array}{c}
u^S_{n_{\bar{s}}} \\ \hline
u^S_{t_{\bar{s}}} \\ \hline
u_r
\end{array}\right\}
=
\left\{\begin{array}{c}
P_{n_{\bar{s}}} + P^F_{n_{\bar{s}}} \\ \hline
P_{t_{\bar{s}}} + P^F_{t_{\bar{s}}} \\ \hline
P_r
\end{array}\right\}
\qquad (43)
$$

where

$u^S_{n_{\bar{s}}}$ = structural displacement components normal to the fluid-structure boundary.

$u^S_{t_{\bar{s}}}$ = structural displacement components tangent to the fluid-structure boundary

u_r = structural displacement components for the remainder of the structure, i.e., those degrees of freedom describing the structure which are not included in $[u^S_{n_{\bar{s}}} \mid u^S_{t_{\bar{s}}}]$.

$[M^S]$ = structural mass matrix

$[K^S]$ = structural stiffness matrix

$P_{n_{\bar{s}}}$, $P_{t_{\bar{s}}}$, P_r = applied external loads (measured from static equilibrium) which do work through the conjugate structural degrees of freedom $u^S_{n_{\bar{s}}}$, $u^S_{t_{\bar{s}}}$, u^S_r ; respectively.

$P^F_{n_{\bar{s}}}$, $P^F_{t_{\bar{s}}}$ = loads produced by the fluid (measured from static equilibrium) which do work through the conjugate structural degrees of freedom $u^S_{n_{\bar{s}}}$, $u^S_{t_{\bar{s}}}$, u^S_r ; respectively.

Equation (43) differs from that of the standard structural mechanics finite element formulation only in the additional loading terms $P^F_{n_{\bar{s}}}$ and $P^F_{t_{\bar{s}}}$ due to the

coupling at the fluid-structure boundary. Since viscous effects in the fluid are neglected*, we have the structural boundary conditions

$$\{P^F_{t_{\bar{r}}}\} = 0 \tag{44a}$$

$$\{P^F_{n_{\bar{r}}}\} = \int_{\tilde{S}_{\bar{r}}} \tilde{p} \, d\,S \tag{44b}$$

where $\tilde{S}_{\bar{r}}$ is the area associated with structural degree of freedom $u^S_{n_{\bar{r}}}$ and $\tilde{p}$ is the fluid pressure adjacent to the displaced fluid-structural boundary. Differences in the Eulerian description of the fluid and the Lagrangran description of the structure requires a treatment similar to that leading to (32) in order to define $\tilde{p}$, see sketch below.

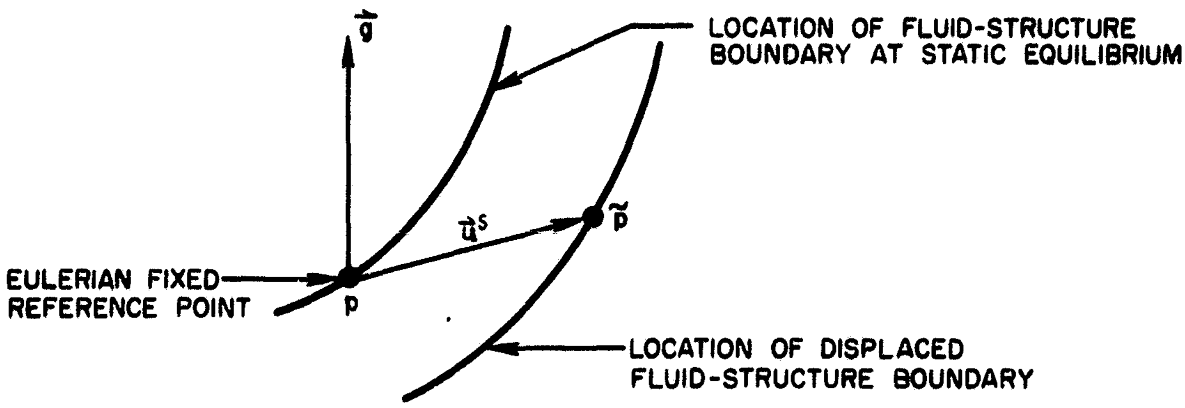

Expanding about p and neglecting higher order terms, we have

$$\tilde{p} = p - \rho\,\vec{g}\cdot\vec{u}^S \tag{45}$$

Writing $\vec{g}$ and the structural displacement vector $\vec{u}^S$ in terms of their components normal and tangential to the original surface and substituting into (44b), we obtain

* See references (1) and (2) for suggested methods of including these effects.

$$\{P^F_{n_{\tilde{s}}}\} = \int_{\tilde{S}_{\tilde{s}}} [p - \rho\, g_t\, u^S_t - \rho\, g_n\, u^S_n]\; dS \tag{46}$$

Equation (46) must now be put into a form suitable for use in a general matrix statement of the hydroelastic problem. As was done in presenting (40) and (41), we shall again symbolically indicate the discretization process associated with (46) and write this in the form

$$\{P^F_{n_{\tilde{s}}}\} = [A]\,\{p_s\} - [K_{n_{\tilde{s}}} \;\vdots\; K_{t_{\tilde{s}}}] \begin{Bmatrix} u^S_{n_{\tilde{s}}} \\ \hline u^S_{t_{\tilde{s}}} \end{Bmatrix} \tag{47}$$

where [A] has been introduced before and [K] is a rectangular matrix reflecting the differences in Eulerian and Lagrangian description. The [K] matrix is a function of gravity.

Equation (47) may now be included in the general matrix statement of the structural problem. Noting that the [K] matrix in (47) has the form of a structural stiffness coefficient, we may write (43) in the form

$$\left[\begin{array}{c:c:c} M^S_{n_{\tilde{s}} n_{\tilde{s}}} & M^S_{n_{\tilde{s}} t_{\tilde{s}}} & M^S_{n_{\tilde{s}} r} \\ \hdashline M^S_{n_{\tilde{s}} t_{\tilde{s}}} & M^S_{t_{\tilde{s}} t_{\tilde{s}}} & M^S_{t_{\tilde{s}} r} \\ \hdashline M^S_{n_{\tilde{s}} r} & M^S_{t_{\tilde{s}} r} & M_{rr} \end{array}\right] \left\{\begin{array}{c} \ddot{u}^S_{n_{\tilde{s}}} \\ \hdashline \ddot{u}^S_{t_s} \\ \hdashline \ddot{u}_r \end{array}\right\} + \left[\begin{array}{c:c:c} K^S_{n_{\tilde{s}} n_s} - K_{n_s} & K^S_{n_{\tilde{s}} t_s} - K_{t_{\tilde{s}}} & K^S_{n_s r} \\ \hdashline K^S_{n_{\tilde{s}} t_s} & K^S_{t_{\tilde{s}} t_{\tilde{s}}} & K^S_{t_{\tilde{s}} r} \\ \hdashline K^S_{n_s r} & K^S_{t_{\tilde{s}} r} & K^S_{rr} \end{array}\right] \left\{\begin{array}{c} u^S_{n_s} \\ \hdashline u^S_{t_s} \\ \hdashline u_r \end{array}\right\} = \left\{\begin{array}{c} P_{n_s} + [A]\,\{p_s\} \\ \hdashline P_{t_s} \\ \hdashline P_r \end{array}\right\} \tag{48}$$

Coupled Fluid-Structure Description – Finite Element

By combining the matrix equations (42) and (48) representing, respectively, the fluid and the structure; we obtain the final system of equations describing the hydroelastic problem.

$$
\begin{bmatrix}
M^F_{ii} & M^F_{if} & M^F_{is} & & & \\
M^F_{if} & M^F_{ff}+M & M^F_{fs} & & & \\
M^F_{is} & M^F_{fs} & M^F_{ss} & A^T & & \\
 & & & M^S_{n_g n_g} & M^S_{n_g t_g} & M^S_{n_g r} \\
 & & & M^S_{n_g t_g} & M^S_{t_g t_g} & M^S_{t_g r} \\
 & & & M^S_{n_g r} & M^S_{t_g r} & M^S_{rr}
\end{bmatrix}
\begin{Bmatrix} \ddot{p}_i \\ \ddot{p}_f \\ \ddot{p}_s \\ \ddot{u}^S_{n_g} \\ \ddot{u}^S_{t_g} \\ \ddot{u}_r \end{Bmatrix}
+
\begin{bmatrix}
K^F_{ii} & K^F_{if} & K^F_{is} & & & \\
K^F_{if} & K^F_{ff} & K^F_{fs} & & & \\
K^F_{is} & K^F_{fs} & K^F_{ss} & & & \\
 & & -A & K^S_{n_g n_g} - K_{nn} & K^S_{n_g t_g} - K_{ts} & K^S_{n_g r} \\
 & & & K^S_{n_g t_g} & K^S_{t_g t_g} & K^S_{t_g r} \\
 & & & K^S_{n_g r} & K^S_{t_g r} & K^S_{rr}
\end{bmatrix}
\begin{Bmatrix} p_i \\ p_f \\ p_s \\ u^S_{n_g} \\ u^S_{t_g} \\ u_r \end{Bmatrix}
=
\begin{Bmatrix} 0 \\ 0 \\ 0 \\ P_{n_g} \\ P_{t_g} \\ P_r \end{Bmatrix}
\quad (49)
$$

Equation (49) is symbolic of the general unsymmetric system of finite element equations describing the hydroelastic problem. A discussion of the problem types considered by the NASTRAN hydroelastic analyzer and the various possible problem solution types is given in the following section.

GENERAL DESCRIPTION OF NASTRAN HYDROELASTIC ANALYZER

The previous derivations have been rather general in nature and applicable to any fluid and/or structural topology consistent with the limiting assumptions. The intent has been to provide a general overview of the theory employed by the program for the solution of the hydroelastic problem. While general methods have been indicated, the details of implementation are not given since this would be beyond the scope of the present report. The details of this implementation are fully discussed in references (1) and (2).

It is the purpose of the present section to briefly specify the problem type treated by NASTRAN, indicate the general input/output data associated with the program, and describe the fluid finite element properties used.

The program has been written to treat the case of axisymmetric fluid volumes (axisymmetric in both geometry and fluid properties) held in elastic containers. However, neither the elastic properties of the structure or the motions of the coupled fluid-structure system need be axisymmetric. Several sample fluid topologies which could be treated by the program are shown in Figure 1.

The NASTRAN formulation of the hydroelastic problem uses the Fourier coefficients of the pressure in an axisymmetric coordinate system as the independent degrees of freedom for the fluid, and uses the structural grid point displacements

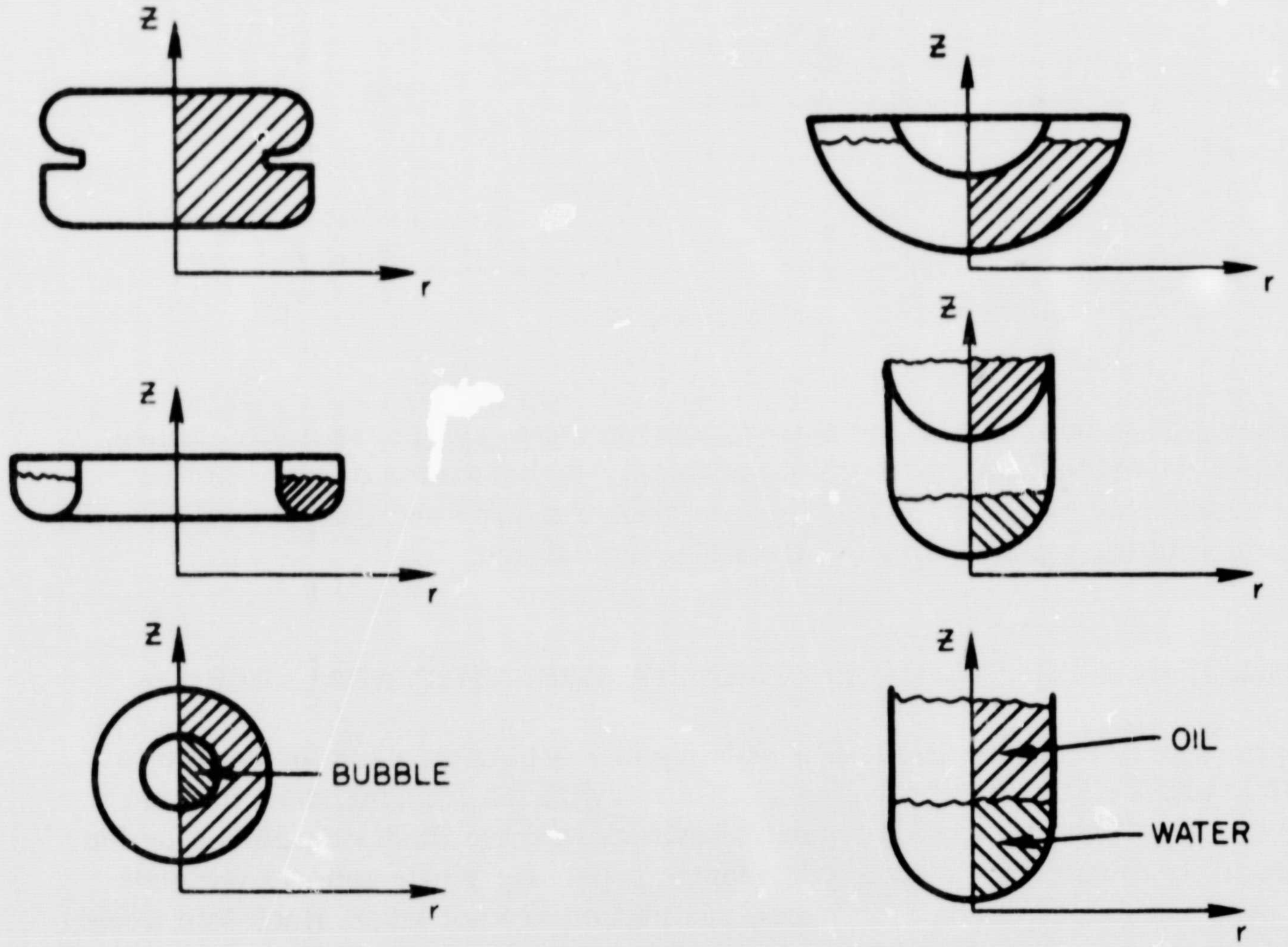

Figure 1. Examples of Permissible Fluid Topologies

and rotations as the independent degrees of freedom for the structure. All NASTRAN structural elements with the exception of the axisymmetric elements (i.e. conic shell, doubly curved shell, and solid of revolution) can be used for the hydroelastic analysis.

Input data to the hydroelastic analyzer associated with the fluid* can be briefly summarized as consisting of the following information:

1. Cross-sectional coordinates of fluid points (fluid circles) – RINGFL cards

2. Connection information and physical properties (ρ and B) for fluid elements connecting fluid points – CFLUIDi cards

3. Identification of structural grid points – GRIDB cards

* Structural input data is basically unchanged from that of the standard NASTRAN as it exists for structural purposes.

4. Sequential list of fluid points on free surfaces and fluid-structure boundaries – FSLIST and BDYLIST cards

5. The harmonic components of fluid pressure to be considered – AXIF cards

6. The magnitude of the gravity vector – AXIF cards

7. Identification of any radial planes of symmetry – FLSYM cards

8. The location of points (r, z, ϕ) on the free surface at which normal displacements are desired for output – FREEPT cards

9. The location of points (r, z, ϕ) in the fluid at which values of the pressure are desired for output – PRESPT cards

10. Direct input matrix terms coupling fluid degrees of freedom with each other or with any structural degree of freedom or extra points - DMIAX cards.

The above input data will be discussed in more detail below. The axisymmetric fluid volume is described by the analyst using a number of concentric circular rings (equivently "fluid points") distributed through the fluid volume and connected by fluid elements having the properties of bulk modules and density, see Figure 2. The user defines the location of the various rings in the fluid volume by specifying the location of the intersection point (fluid point) of the ring with an arbitrary transverse r-z plane containing the axis of symmetry. The fluid point locations are given in either a cylindrical or spherical coordinate system on the RINGFL input data cards while CFLUDi input cards are used to specify fluid element connection data.

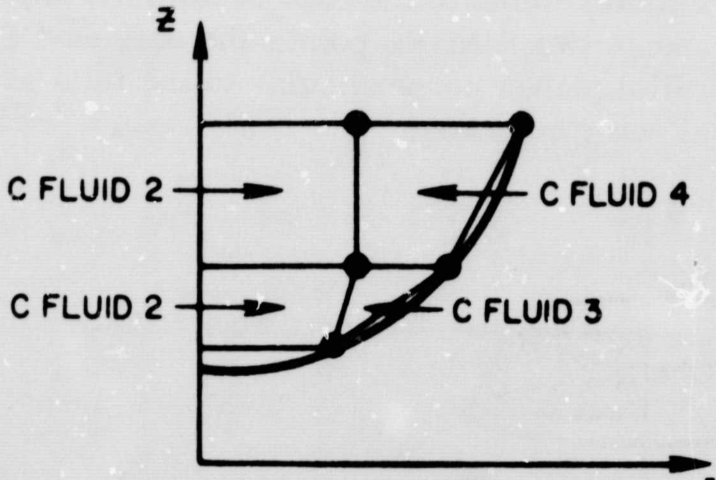

Figure 2. Sample Fluid Model

Three types of fluid elements are provided:

1. CFLUID3 – Triangular element defining an annular volume of triangular cross-section. This element connects three RINGFL points.

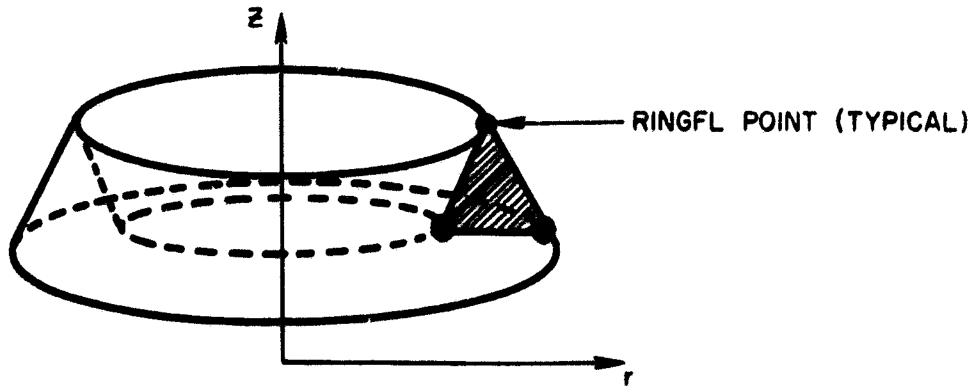

2. CFLUID4 – Quadrilateral element defining an annular volume of quadrilateral cross-section. This element connects four RINGFL points.

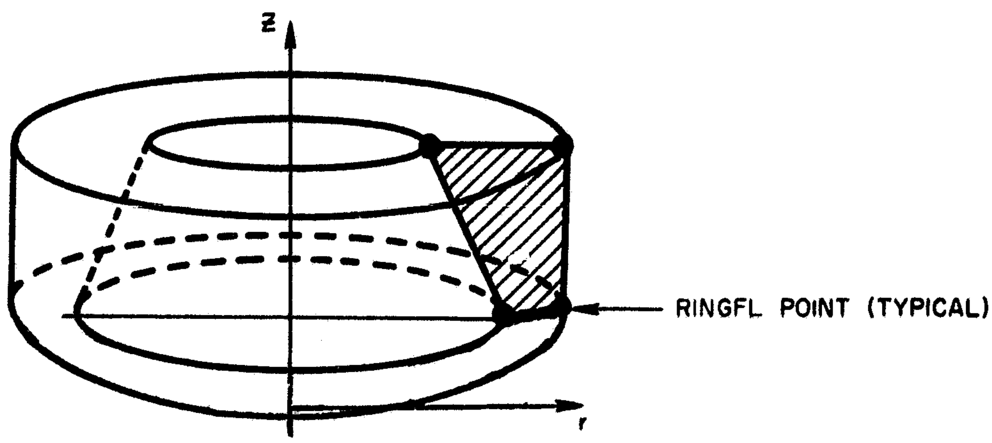

3. CFLUID2 – Center element defining a fluid disk. This element is required to connect a fluid volume to the axis of fluid symmetry. The center element connects two RINGFL points and defines a fluid volume bounded by two parallel planes perpendicular to the fluid axis of symmetry and a conical outer boundary.

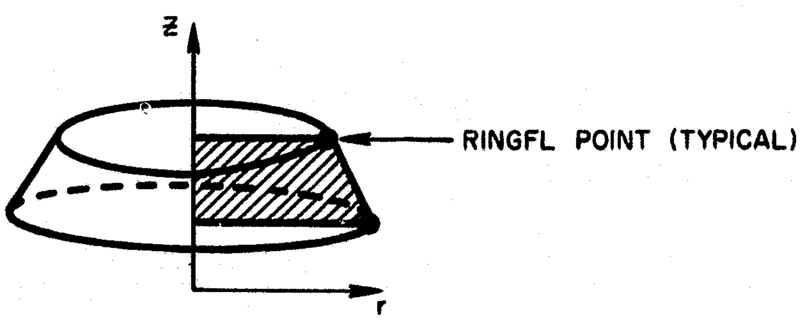

Figure 2 shows a sample fluid model utilizing the various fluid elements.

The fluid element properties defining the character of the finite element matrices (i.e. of [a] and [b] of the assembled system) are obtained by expanding the pressure in a Fourier series with respect to the circumferential coordinate ϕ, thus

$$p(r, z, \phi) = \sum_{n=0}^{N} P^n \cos n\phi + \sum_{n=1}^{N} P^{n*} \sin n\phi \tag{50}$$

where P^n and P^{n*} are functions of the axial (z) and radial (r) coordinates. Assuming, in turn, a functional relation over the r,z cross-section of the fluid element in terms of generalized coordinates q_j^n and q_j^{n*}, we can write

$$\begin{aligned} P^n &= P^n(r, z) = [L^n(r, z)] \cdot \{q_j^n\} \quad n \geq 0 \\ P^{n*} &= p^{n*}(r, z) = [L^n(r, z)] \cdot \{q_j^{n*}\} \quad n \geq 1 \end{aligned} \tag{51}$$

Here the matrix $[L^n]$ reflects the assumed pressure distribution over the element cross-section, and the generalized coordinates are chosen so that the values of P^n and P^{n*} match the values of the pressure coefficients at the fluid points located at the corners of the element. Thus, if P_i^n is the value of P^n at the i^{th} fluid grid point, we may write

$$\begin{aligned} \{q_j^n\} &= [H_{qp}^n] \cdot \{P_j^n\} \\ \{q_j^{n*}\} &= [H_{qp}^n] \cdot \{P_i^{n*}\} \end{aligned} \tag{52}$$

Substituting (52) and (51) into (50) results in an expression for p in terms of the fluid degrees of freedom P_i^n and P_i^{n*}. This relation is equivalent, on an element level, to equation (19) with p_j designating the fluid element freedoms. The element properties, i.e. generalized mass and stiffness, can then be obtained by the procedure indicated by equations (23) and (24).

From the above discussion, we see that each fluid point has a number of harmonic pressure degrees of freedom associated with it. In this respect we note the similarity with the six degrees of freedom usually associated with a structural grid point in NASTRAN.

The triangular fluid element properties are derived under the assumption that the pressure varies linearly with position over the cross-section described by the triangle. For this case

$$[L^n (r, z)] = [1 \mid r \mid z] \tag{53}$$

and

$$[H^n_{qp}] = \begin{bmatrix} 1 & r_1 & z_1 \\ 1 & r_2 & z_2 \\ 1 & r_3 & z_3 \end{bmatrix}^{-1} \tag{54}$$

where r_i, z_i ($i = 1, 2, 3$) are the coordinates of the three connecting fluid points.

The quadrilateral fluid element properties are obtained by averaging four triangular elements; see sketch below.

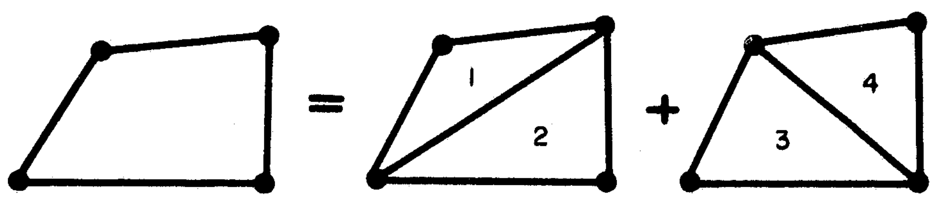

The properties of the center element are derived using an assumed pressure distribution obtained from an asymptotic solution of the wave equation as $r \to 0$. For this case

$$[L^n (r, z)] = [(r)^n \mid (r)^n z] \tag{55}$$

$$[H^n_{qp}] = \left|\begin{array}{c|c} (r_1)^n & (r_1)^n\ z_1 \\ \hline (r_2)^n & (r_2)^n\ z_2 \end{array}\right| \tag{56}$$

where r_i, z_i ($i = 1, 2$) are the coordinates of the two connecting fluid points.

The effects of spatial variations in fluid properties, e.g. the case of oil on water, can be included in the analysis since fluid properties are specified at the element level.

In addition to the RINGFL and CFLUIDi cards already described, additional input Bulk Data Cards provided for the hydroelastic problems are briefly reviewed:

1. The AXIF card describes the fluid coordinate system, the gravity parameter parallel to the axis of fluid symmetry, and a user chosen list of fluid harmonics to be used for the particular problem.

2. The FSLIST and BDYLIST cards describe the fluid boundary. The FSLIST card lists the fluid points which lie on a free surface while the BDYLIST card lists fluid points on a fluid-structure boundary. Fluid boundary points not included on either of the above lists are assumed to lie on a rigid boundary.

3. The PRESPT and FREEPT data cards specify special fluid output points. The PRESPT card specifies locations for pressure output (i.e., in addition to harmonic pressure output). The FREEPT card is used to define locations on the free surface boundary for surface displacement output (see equation (33)).

4. The FLSYM data card allows the user to optionally model portions of the problem with planes of symmetry (symmetric and/or antisymmetric) containing the fluid axis of symmetry.

5. The GRIDB card identifies structural grid points for hydroelastic problems. This card identifies the specified structural grid point with a particular RINGFL fluid point. (It should be noted that the r, z coordinates of each structural grid point on the fluid-structure boundary must coincide with the r, z coordinates of one of the fluid points on the interface.)

6. The DMIAX card allows the user to input special purpose matrices for his particular problem. For example, surface friction effects can be included by methods introduced in references (1) and (2).

From the given input data, the program automatically assembles the hydroelastic problem, including the effects of free surfaces and fluid-structure boundaries, represented by (49). Various solutions associated with (49) may then be requested from the twelve Rigid Formats available within NASTRAN.

The available Rigid Formats are:

#1 - Static Analysis
#2 - Static Analysis with Inertia Relief
#3 - Normal Mode Analysis
#4 - Static Analysis with Differential Stiffness
#5 - Buckling Analysis
#6 - Piecewise Linear Analysis
#7 - Direct Complex Eigenvalue Analysis
#8 - Direct Frequency and Random Response
#9 - Direct Transient Response
#10 - Modal Complex Eigenvalue Analysis
#11 - Modal Frequency and Random Response
#12 - Modal Transient Response

While the fluid effects have been programmed so as to be compatible with all of these, the following characteristics of the hydroelastic problem cause restrictions on the type of non-trivial solutions which may be obtained:

1. The formulation is for dynamic perturbations from static equilibrium.

2. The system of equations (49) describing the general hydroelastic problem is unsymmetric. Since the first six Rigid Formats are restricted to the use of symmetric matrices, the program automatically ignores the fluid-structure boundary. Thus, for these Rigid Formats the program solves the problem of a fluid in a rigid container with an optional free surface (equivalent to (42) with $\{\ddot{u}^S_{\bar{n}_s}\} = \{0\}$) and an uncoupled elastic structure with no fluid present (equivalent to (43) with $\{P^F_{\bar{n}_s}\} = \{P^F_{\bar{t}_s}\} = \{0\}$).

3. The only direct means of exciting a fluid is through the fluid-structure boundary since no means is provided for the direct input of applied loads on the fluid.

With the above restrictions in mind, the suggested Rigid Formats are outlined below:

Rigid Format #3 – The uncoupled modes of a fluid in a rigid container and a structure with no fluid may be found.

Rigid Format #7 – The coupled modes of the fluid and structure may be found.

Rigid Formats #8 and #9 – External loads may be applied to the structural grid points only. For the Direct Transient Analysis, initial conditions may only be given for the structural degrees of freedom since the fluid is assumed to be initially at static equilibrium.

Rigid Formats #10, #11, and #12 – The practicality of these is limited since the modal coordinates used to formulate the dynamic matrices are the normal modes of the fluid and structure solved as uncoupled systems. For widely spaced fluid and structure frequency ranges, however, some utility may exist for these formats.

Upon solution of the particular problem, the program outputs both fluid and structural data. The available structural data is unchanged from the present NASTRAN structural program. Fluid output data which may be directly requested includes fluid harmonic pressures, fluid pressures (PRESPT), and free surface displacements (FREEPT). First and second time derivatives of fluid pressure and free surface displacement may also be obtained. Printed values for the fluid may include real and complex values. Both x-y Plot and random analyses capability are available for FREEPT and PRESPT points.

CONCLUDING REMARKS

A derivation leading to a general finite element statement of the hydroelastic problem has been presented and a description of the NASTRAN hydroelastic analyzer based on this derivation has been given. Some of the more important characteristics of the hydroelastic analyzer are summarized below.

Limiting restrictions:

1. Only small dynamic perturbations from static equilibrium are considered.

2. The fluid must have axisymmetric geometry and properties.

3. Fluid disturbances propagate by an adiabatic process.

4. The fluid is nonviscous.

5. Gravity gradient effects are neglected.

6. If gravity is present, the gravity vector must be parallel to the axis of fluid symmetry and any free surface must lie in a plane perpendicular to this axis.

7. The application of external loads is allowed only on structural grid points.

8. Axisymmetric structural elements cannot be used.

9. The effects of variable fluid density and gravity field are not completely compatible. If the effects of either gravity or variable density are small, they may be used together but second order errors may result.

Capabilities and Characteristics:

1. Motions of both coupled and uncoupled fluid-structural systems may be treated.

2. Rigid and/or elastic structural boundaries can be included.

3. Multiple boundary effects may be analyzed.

4. Effects of variable fluid density and compressibilities may be included.

5. Fluid free-surface effects can be treated.

6. Degrees of freedom of the fluid are the harmonic pressure coefficients.

7. Degrees of freedom of the structure are the grid point displacements and rotations.

8. Fluid behavior is measured from a fixed reference point.

9. Symmetric and antisymmetric capability exists to take advantage of symmetry planes.

10. Fluid description is generally compatible with all NASTRAN system capability.

An experienced user of the program using available NASTRAN features (e.g. Direct Matrix Inputs, Alters, Multi-Point-Constraints, etc.) can circumvent many of the restrictions in the above summary lists. Several examples of this are briefly discussed here.

As has been mentioned previously, viscous effects can be included by the input of a damping matrix to (49) for the inclusion of viscous wall friction. Additionally, sources and/or sinks in fluids without free surfaces could be treated by the addition of "generalized body forces" at the source/sink points. Also, one and two dimensional Laplacian fluid elements, obtained from existing NASTRAN scalar and membrane elements by procedures explained in reference (6), could be used in conjunction with the CFLUIDi elements for treating certain fluid problems*.

The NASTRAN hydroelastic analyzer should provide a powerful analytical tool. The present program capability of control system modeling can be included to yield a description of coupled fluid-structure-control system problems. The direct application of the program to many acoustics problems is obvious.

* It should be noted that one and two-dimensional Laplacian elements could be used "stand-alone" to treat many problems if care is taken in the choice of generalized mass and boundary terms. Also, with this approach, velocity potential, steam functions, pressure, etc. could be taken as the fluid freedoms.

REFERENCES

1. Herting, D. N., MacNeal, R. H., and Longacre, H. L., "NASTRAN Hydroelastic Theoretical Development and Functional Module Mathematical Specifications," MS 84-2, March 1970.

2. MacNeal, R. H., "NASTRAN Theoretical Manual," (hydroelastic additions to be available about January 1, 1972), NASA Publications SP-221.

3. Zienkiewicz, O. C. and Cheung, Y. K., The Finite Element Method in Structural and Continuum Mechanics. McGraw-Hill Publishing Co., Ltd., 1967.

4. Berg, P. W., "Calculus of Variations," Handbook of Engineering Mechanics, edited by Flugge, W., McGraw-Hill Book Company, Inc., 1962.

5. Przemieniecki, J. S., The Theory of Matrix Structural Analysis, McGraw-Hill, 1968.

6. Mason, J. B., "The Solution of Heat Transfer Problems by the Finite Element Method Using NASTRAN," NASA X-321-70-97, 1970.

APPENDIX A

This material is taken directly from the NASTRAN Demonstration Problem Manual and shows a comparison between hydroelastic analyzer and theoretical results for several sample problems.

RIGID FØRMAT No. 3, Real Eigenvalue Analysis
Vibration of a Compressible Gas in a Rigid Spherical Tank (3-2)

A. Description

This problem demonstrates a compressible gas in a rigid spherical container. In NASTRAN a rigid boundary is the default for the fluid and, as such, no elements or boundary lists are necessary to model the container.

Aside from the NASTRAN bulk data cards currently implemented, this problem demonstrates the use of the hydroelastic data cards: AXIF, CFLUID2, CFLUID3, and RINGFL.

The lowest mode frequencies and their mode shapes for n = 0, 1 and 2 are analyzed where n is the Fourier harmonic number. Only the cosine series is analyzed.

B. Model

1. Parameters

$R = 10.0$ m	(Radius of sphere)
$\rho = 1.0 \times 10^{-3}$ Kg/m^3	(Mass density of fluid)
$B = 1.0 \times 10^{3}$ Newton/m^2	(Bulk modulus of fluid)

2. Figure 1 and 2 show the finite element model. The last 3 digits of the RINGFL identification number correspond approximately to the angle, θ, from the polar axis along a meridian.

C. Theory

From Reference 18, the pressure in the cylinder is proportional to a series of functions:

$$Q_{n,m} = \frac{J_{m+\frac{1}{2}}(X)}{\sqrt{X}} P_m^n (\cos\theta) \cos n\phi , \qquad \begin{matrix} n \le m \\ m = 0,1,2 \end{matrix} \tag{1}$$

where:

$Q_{n,m}$	Pressure coefficient for each mode
X	Nondimensional radius $= \frac{\omega_{mk}}{a} r$
ω_{mk}	Natural frequency for the kth mode number and mth radial number in radians per second
$J_{m+\frac{1}{2}}$	Bessel function of the first kind

r radius

$a = \sqrt{\frac{B}{\rho}}$ speed of sound in the gas

P_m^n associated Legendre functions

θ meridinal angle

ϕ circumferential angle

n harmonic number

m number of radial node lines

The solution for X and hence ω_{mk} is found by the use of the boundary condition that the flow through the container is zero.

$$\left\{\frac{d}{dX}\left[\frac{J_{m+\frac{1}{2}}(X)}{\sqrt{X}}\right]\right\}_{r=R} = 0.0 \qquad (2)$$

where R is the outer radius.

This results in zero frequency for the first root. Multiple roots for other modes can be seen in Table 1. The finite element model assumes different pressure distributions in the two angular directions which causes the difference in frequencies.

D. <u>Results</u>

Table 1 and Figure 3 summarize the NASTRAN and analytic results for the lowest nonzero root in each harmonic. Table 1 lists the theoretical natural frequencies, the NASTRAN frequencies, the percent error in frequency, and the maximum percent error in pressure at the wall as compared to the maximum value. Figure 3 shows the distribution of the harmonic pressure at the wall versus the meridinal angle. The theoretical pressure distributions correspond to the Legendre functions P_o^0 (cos θ), P_o^1 (cos θ), and P_o^2 (cos θ) which are proportional to cos θ, sin θ, and $\sin^2\theta$ respectively.

Table 1. Comparison of NASTRAN and analytical results.

Harmonic	Natural Frequency (Hertz)			Pressure
	Analytical	NASTRAN	% Error	Max. % Error at Wall
0	33.1279	33.2383	0.33	1.19
1	33.1279	33.2060	0.24	0.47
2	53.1915	53.3352	0.27	0.91

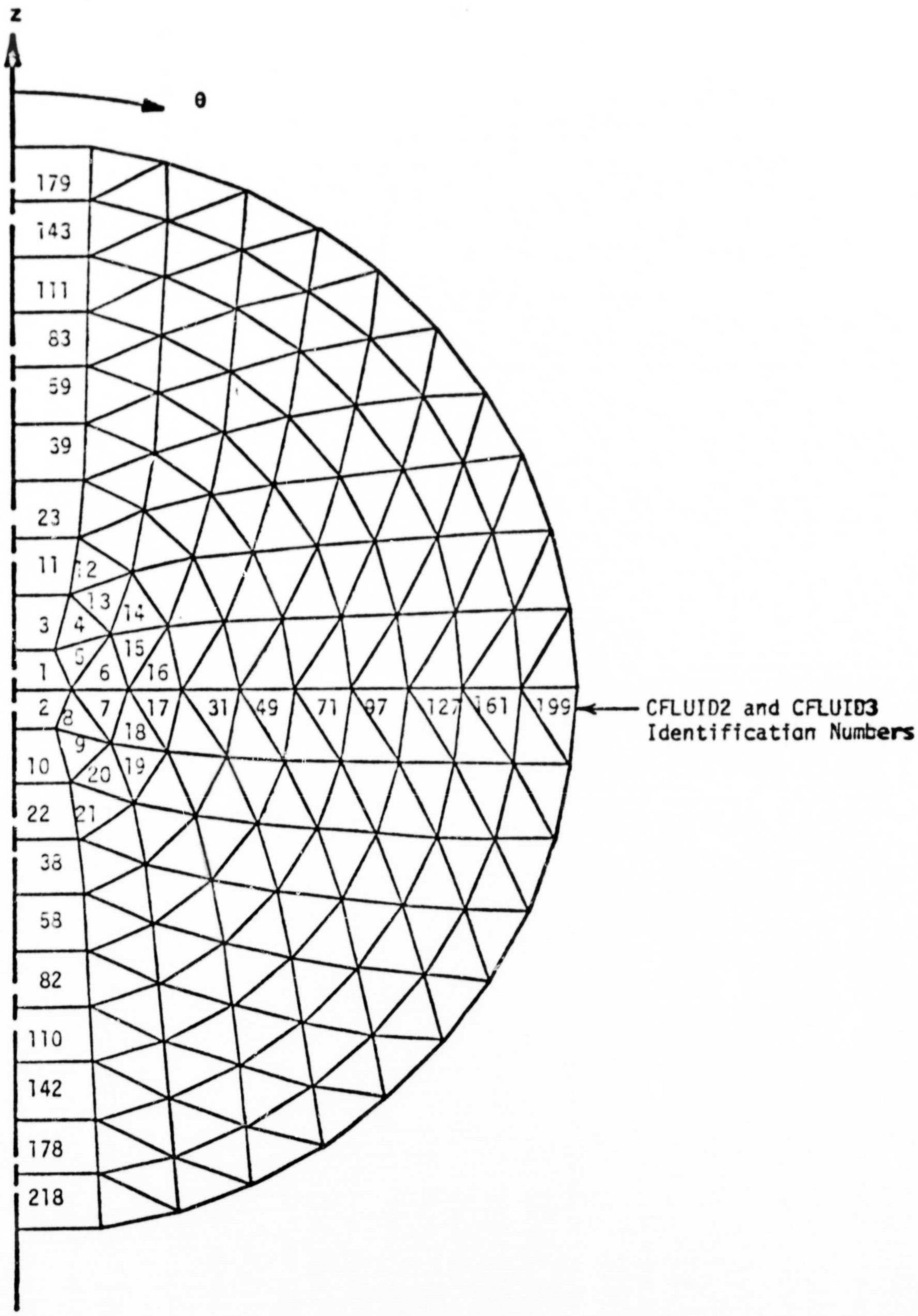

Figure 1. Gas filled rigid spherical tank model.

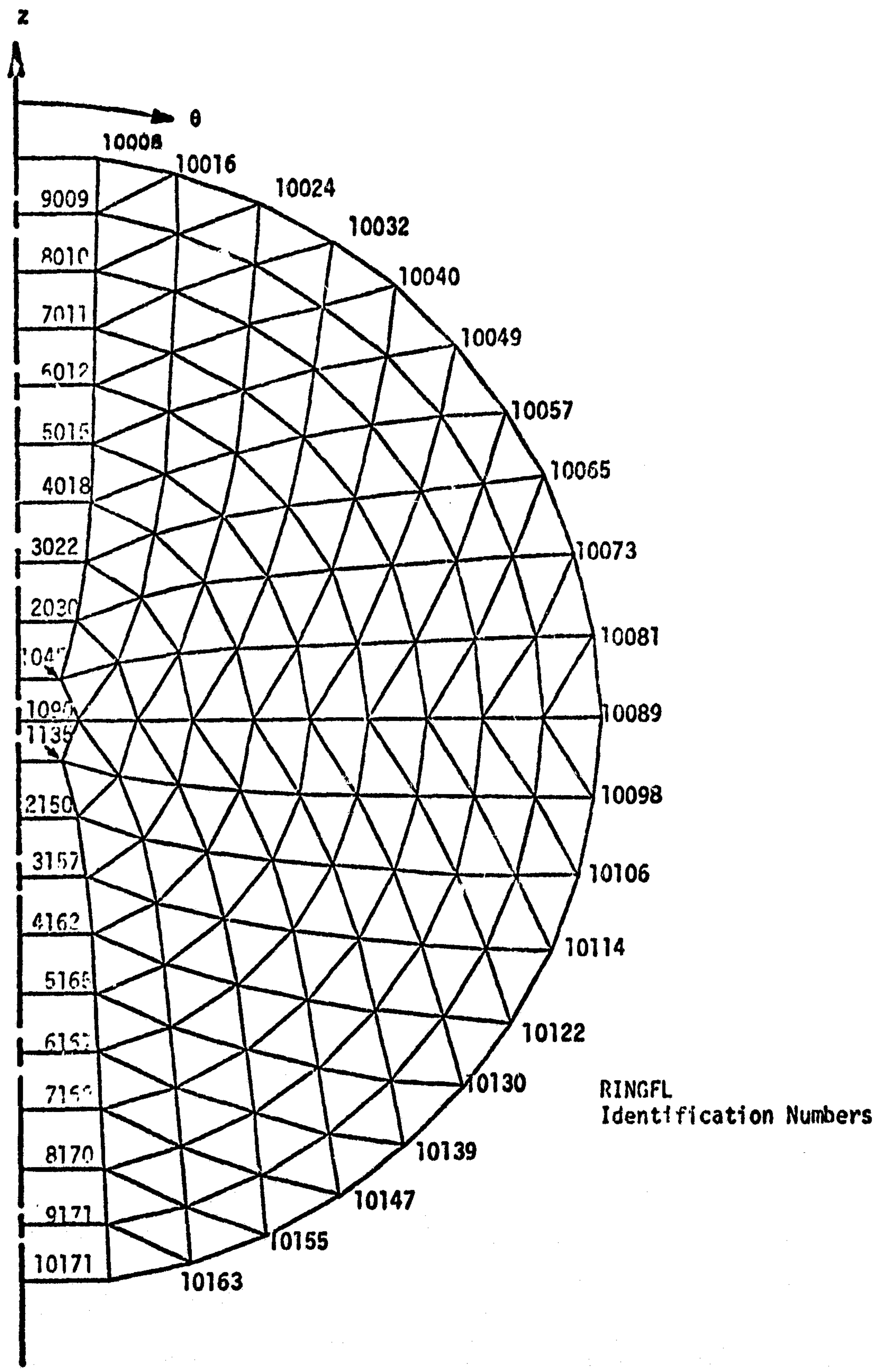

Figure 2. Gas filled rigid spherical tank model.

3.2-5 (9/1/70)

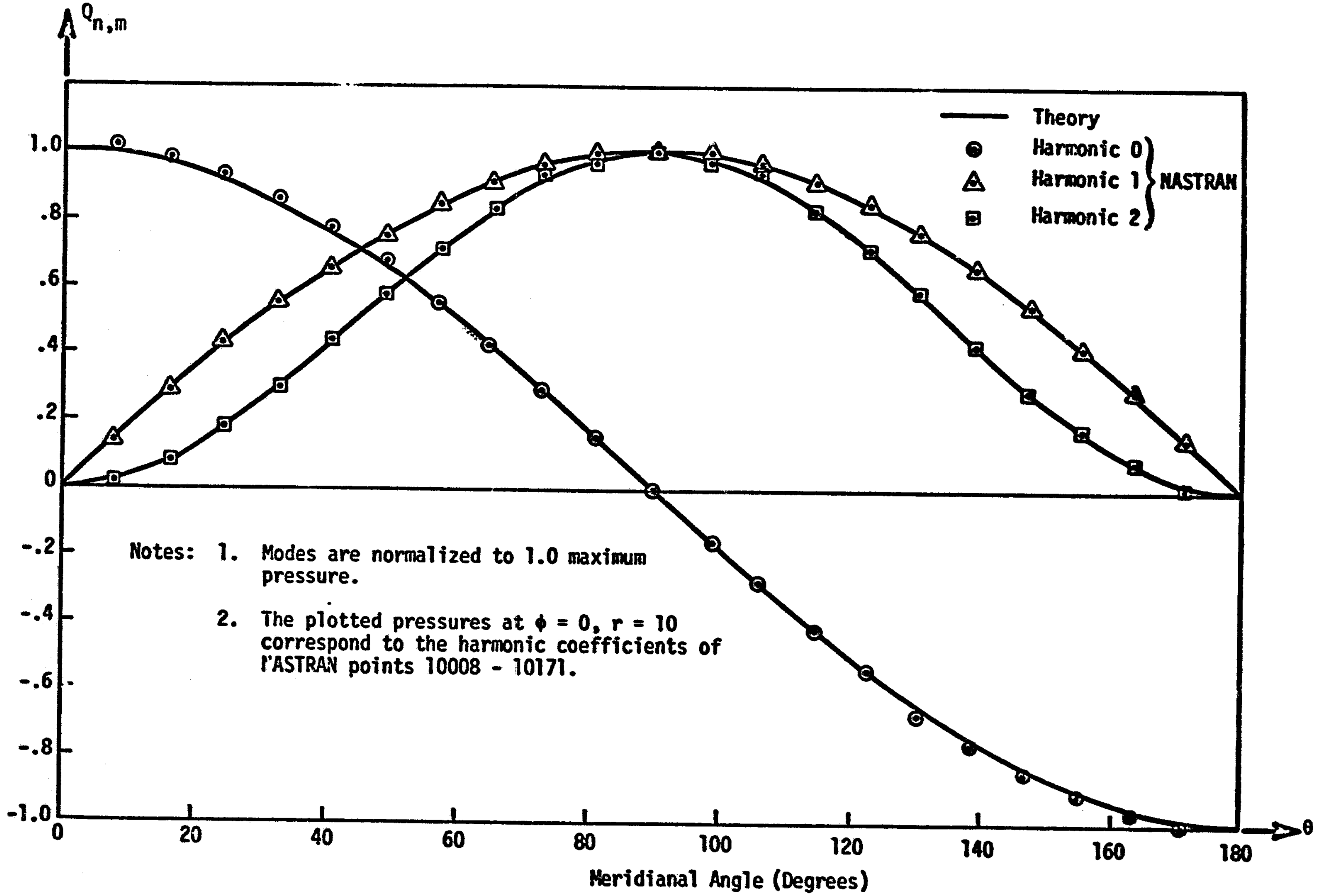

Figure 3. Pressure at tank wall - first finite modes.

RIGID FORMAT No. 3, Real Eigenvalue Analysis
Vibration of a Liquid in a Half Filled Rigid Sphere (3-3)

A. Description

The model is similar to Demonstration Problem No. 3-2 except that a hemispherical fluid model with a free surface is analyzed. Additional cards demonstrated are the free surface list (FSLIST) and free surface points (FREEPT). The effective gravity for the fluid is found on the AXIF card. The fluid is considered incompressible.

The lowest three eigenvalues and eigenvectors for the cosine and sine series of $n = 1$ are analyzed, where n is the harmonic order.

B. Input

1. Parameters

g =	10.0 ft/sec^2	(Gravity)
R =	10.0 ft	(Radius of hemisphere)
ρ =	1.255014 lb-sec^2/ft^4	(Fluid mass density)
B =	∞	(Bulk modulus of fluid, incompressible)

2. Figure 1 shows the finite element model.

C. Results

Reference 17 gives the derivations and analytical results. In particular, the parameters used in the reference are:

$$\left.\begin{aligned} e &= 0 \quad \text{(half-filled sphere)} \;, \\ \lambda &= \frac{\omega^2 R}{g} \text{ (dimensionless eigenvalue)} \;. \end{aligned}\right\} \quad (1)$$

Table 2 of Reference 17 lists the eigenvalues, λ_1, λ_2, and λ_3 for the first three modes. Figure 13 of Reference 17 shows the mode shapes.

The analytic and NASTRAN results are compared in Table 1. The frequencies are listed and the resulting percentage errors are given. The maximum percent error of the surface displacement, relative to the largest displacement, is tabulated for each mode.

The free surface displacements may be obtained by the equation:

$$u = \frac{p}{\rho g} \quad , \tag{2}$$

where p is the pressure at the free surface recorded in the NASTRAN output. Note that, since an Eulerian reference frame is used, the pressure at the original (undisturbed) surface is equal to the gravity head produced by motions of the surface. Special FREEPT data cards could also have been used for output. Since the results are scaled for normalization anyway, the harmonic pressures may be used directly as displacements.

Figure 2 is a graph of the shape of the free surface for each distinct root. Both analytic and NASTRAN results are scaled to unit maximum displacements. Because the cosine series and the sine series produce identical eigenvalues, the resulting eigenvectors may be linear combinations of both series. In other words the points of maximum displacement will not necessarily occur at $\phi = 0°$ or $\phi = 90°$. Since the results are scaled, however, and the results at $\phi = 0$ are proportional to the results at any other angle, the results at $\phi = 0$ were used.

Table 1. Comparison of natural frequencies and free surface mode shapes from the reference and NASTRAN.

Mode Number	Natural Frequency (Hertz)			Mode Shape
	Reference	NASTRAN	NASTRAN % Error	Maximum % Error, ε
1	0.1991	0.1988	-0.1	ε < 1 %
2	0.3678	0.3691	0.3	ε < 2.6%
3	0.4684	0.4766	1.8	ε < 4 %

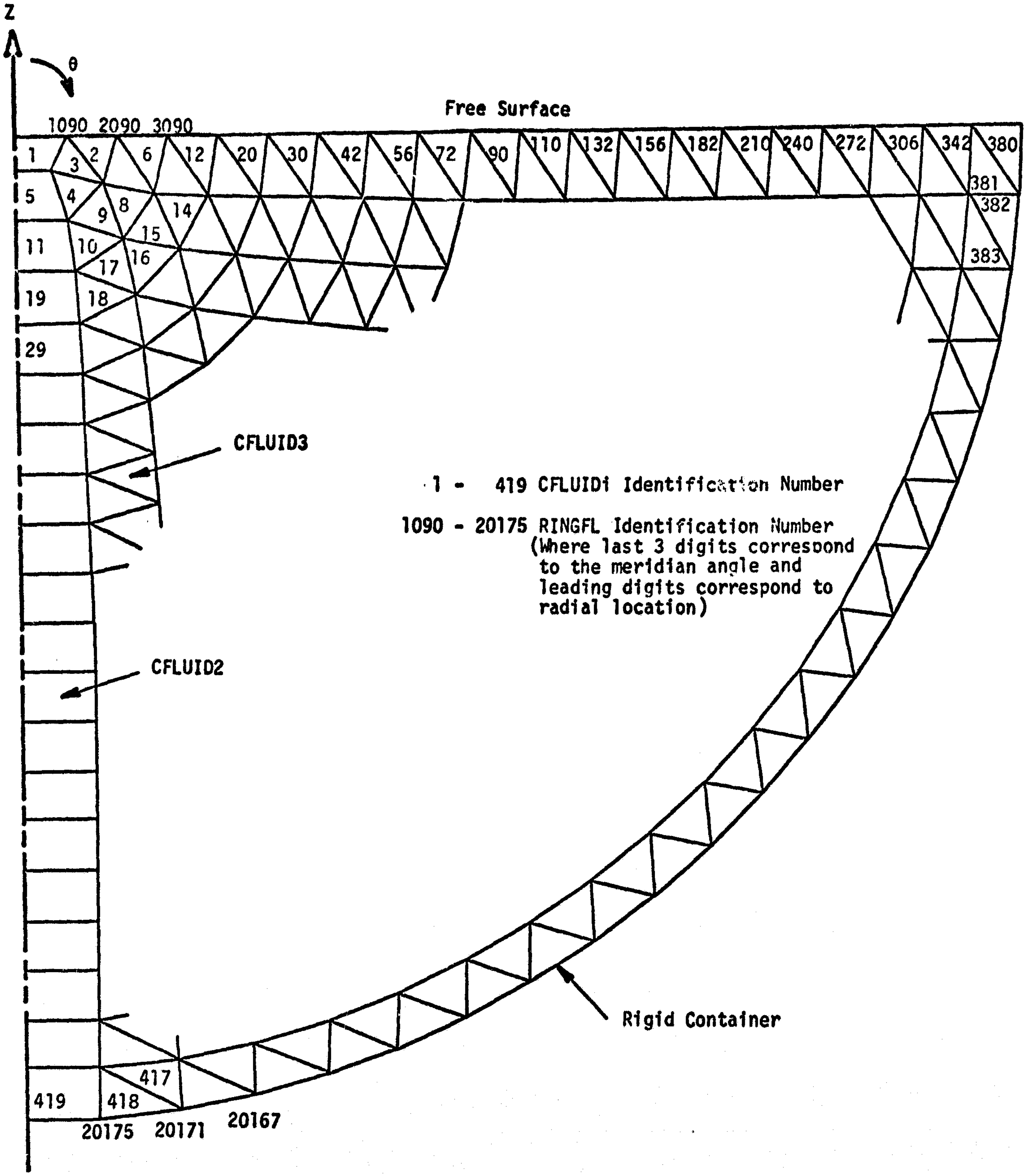

Figure 1. Rigid sphere half filled with a liquid.

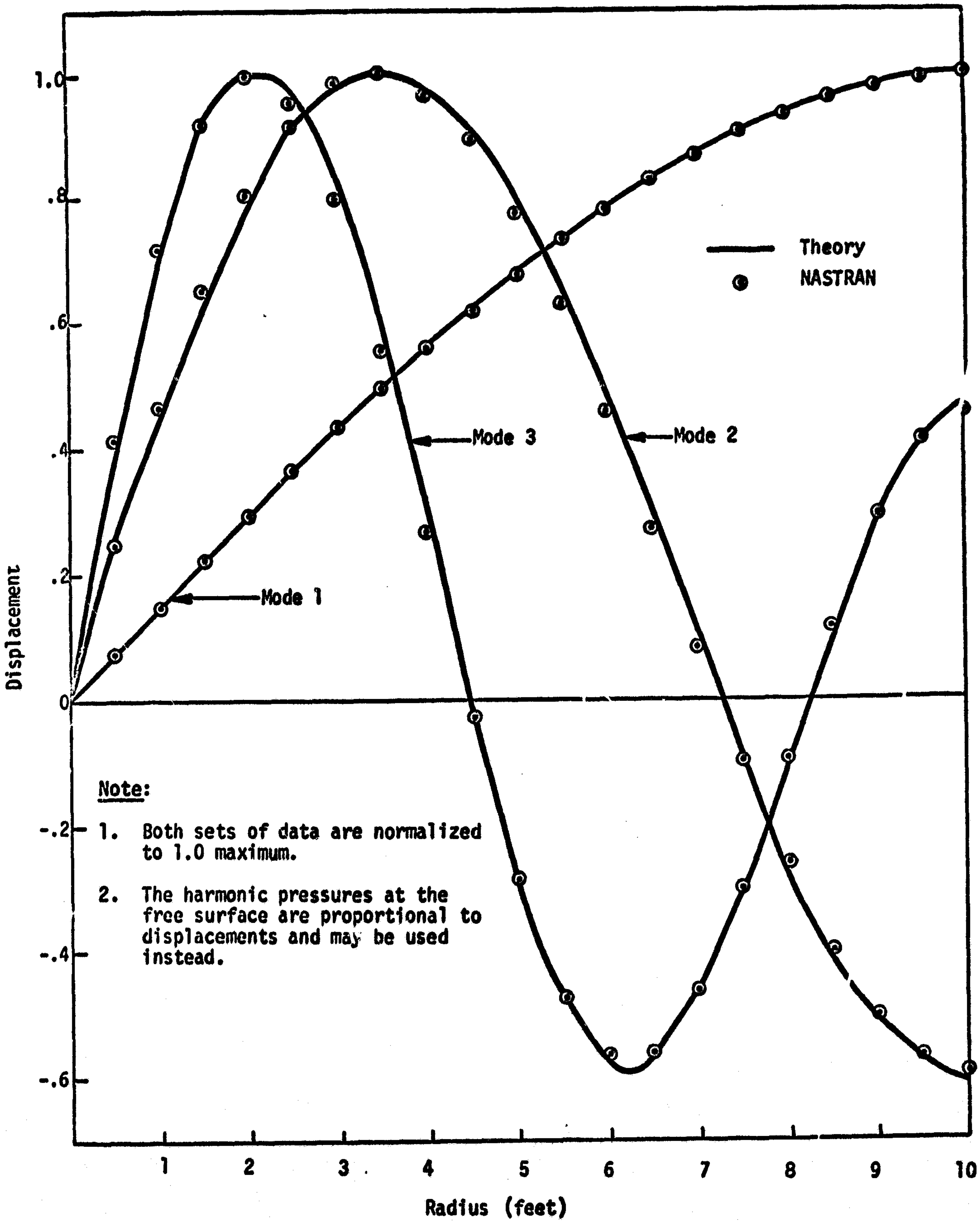

Figure 2. Free surface mode shapes.

RIGID FORMAT No. 7, Complex Eigenvalue Analysis - Direct Formulation
Complex Eigenvalue Analysis of a Gas-Filled Thin Elastic Cylinder (7-2)

A. Description

This problem demonstrates the use of symmetry to analyze specific harmonics of a fluid-filled structure. The problem to be solved consists of a cylindrical section filled with a compressible fluid. The end conditions for the cylinder and the fluid are two planes of antisymmetry, perpendicular to the axis. These end conditions correspond to the conditions that exist at periodic intervals along a long, fluid-filled pipe vibrating in one of its vibration modes. The antisymmetric boundary for the structure is defined by constraining the motions which lie in the plane. An antisymmetric boundary for the fluid corresponds to zero pressure. This may be modeled, in NASTRAN, by defining the plane of antisymmetry as a free surface with zero gravity.

The lowest natural frequencies and mode shapes for the third and fifth harmonics are analyzed separately. For the third harmonic, the structure is defined by a section of a cylinder having an arc of 30 degrees or 1/12 of a circle. The fifth harmonic analysis uses a section having an arc of 18 degrees or 1/20 of a circle. The longitudinal edges, which were cut, are planes of symmetry and antisymmetry in order to model a quarter cosine wave length.

The bulk data cards used are; AXIF, BDYLIST, CFLUID2, CFLUID4, CØRD2C, CQUAD1, EIGC, FLSYM, FSLIST, GRIDB, MAT1, PQUAD1, RINGFL, and SPC1.

B. Input

The finite element model for the third harmonic is shown in Figures 1 and 2. Parameters used are:

$B = 2.88 \times 10^3$ lb/in^2	(Bulk modulus of fluid)
$\rho_f = 1.8 \times 10^{-2}$ lb-sec^2/in^4	(Fluid mass density)
$\rho_s = 6.0 \times 10^{-2}$ lb-sec^2/in^4	(Structure mass density)
$E = 1.6 \times 10^5$ lb/in^2	(Young's modulus for structure)
$G = 6.0 \times 10^4$ lb/in^2	(Shear modulus for structure)

$a = 10.0$ inch (Radius of cylinder)

$\ell = 10.0$ inch (Length of cylinder)

$h = 0.01$ inch (Thickness of cylinder)

The model for the fifth harmonic is similar to the third harmonic model except that the angle covered by the structure is 18° instead of 30°. This is accomplished by simply removing the structural elements and boundary GRIDB points corresponding to the two right-hand layers of structure (between 18° and 30°). The FLSYM, FSLIST and SPC1 cards are changed to reflect the 1/20 symmetry.

C. Theory

The derivations and results for this problem are described in Reference 16. The results for various dimensionless parameters are listed. The particular parameters for the problem at hand are:

$$\eta = \frac{\rho_f a}{\rho_s h} = 300.0 \quad ,$$

$$C = \sqrt{\frac{G\rho_f}{B\rho_s}} = 2.5 \quad ,$$

$$\Omega = \frac{P_o a}{Gh} = 0.0 \quad ,$$

where η is the ratio of fluid mass to structure mass. C is the ratio of the wave velocity in the structure material to the wave velocity in the fluid. Ω is the factor describing static pressurization, P_o.

The basic assumptions for this analysis are:

1. Thin shell theory is used for the structure. The bending moment terms in the force equilibrium equations are ignored in the results.

2. The fluid is nonviscous, irrotational, and small motions are only considered.

This particular problem becomes relatively easy to solve since the mode shapes for the fluid in a rigid container and the modes of the structure with no enclosed fluid have the same spatial function at the interface. Each mode of the fluid is excited by only one mode of the structure and each mode of the structure is excited by one mode of the fluid. The pressure in the fluid is

assumed to be a series of functions:

$$P = P_n e^{i\omega t} \cos n\phi \ \sin \frac{\pi z}{\ell} Q_n(r,\omega) \quad , \tag{1}$$

where Q_n is a Bessel Function or a modified Bessel Function of the first kind.

The characteristic shapes of the structure are a series of the form:

$$u = A e^{i\omega t} \cos n\phi \ \sin \frac{\pi z}{\ell} \quad , \tag{2}$$

where u is the displacement normal to the surface. The fundamental momentum equation for the fluid flow at the boundary is:

$$\nabla(P(r))\cdot\vec{e}_r = -\rho_f \ddot{u} \quad , \tag{3}$$

where $\vec{e}_r$ is a unit vector in the radial direction.

The forces on the structure at the boundary are:

$$P(a) = \frac{1}{a}\frac{\partial^2 F_1}{\partial z^2} - \rho_s h\ddot{u} \quad , \tag{4}$$

where the function F_1 is defined by the differential equation on the surface:

$$\nabla^4 F_1 = \frac{Eh}{a}\frac{\partial^2 u}{\partial z^2} \quad . \tag{5}$$

The solution for F_1 is obtained by assuming that

$$F_1 = B e^{i\omega t} \cos n\phi \ \sin\frac{\pi z}{\ell} \quad . \tag{6}$$

Combining Equations 1 through 6 results in the relationships:

$$\rho\omega^2 A = P_n \left.\frac{\partial Q_n(r,\omega)}{\partial r}\right|_{r=a} \tag{7}$$

$$Q_n(a,\omega) P_n = \left[\frac{a^2\pi^4 Eh}{\ell^4\left(\frac{\pi^2 a^2}{\ell^2} + n^2\right)^2} + \rho_s h\omega^2\right] A \tag{8}$$

Equation (7) is a statement of the continuity of displacement. Equation (8) states the balance of the pressures. The above equations may be solved by iterating on ω. Reference 16 provides solutions for ω over a wide range of parameters.

D. Results

The analytic and NASTRAN eigenvalues are listed in Table 1. The corresponding errors in the eigenvalues are tabulated and the maximum errors in displacement at the container wall are given as the percentage of the maximum value. The container displacements in the radial direction at $\phi = 0.0$ are compared in Figure 3.

Table 1. Comparison of analytical and NASTRAN results.

Harmonic	Natural Frequency (Hertz)			Mode Shape
	Analytical	NASTRAN	% Error	Max. % Error in Radial Displ.
3	1.579	1.595	1.0	~0.0
5	1.011	1.049	3.4	0.5

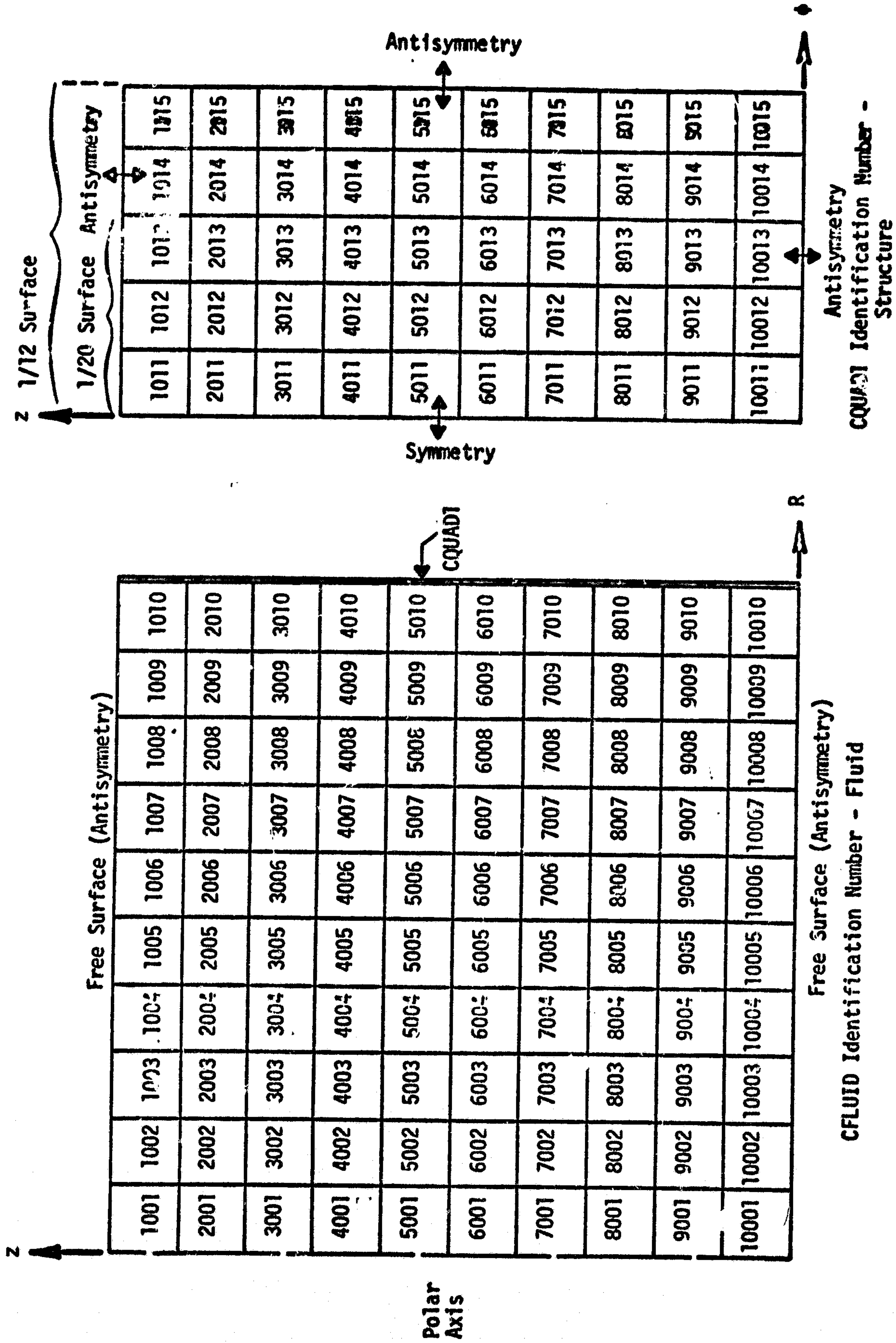

Figure 1. Elastic cylinder and gas model.

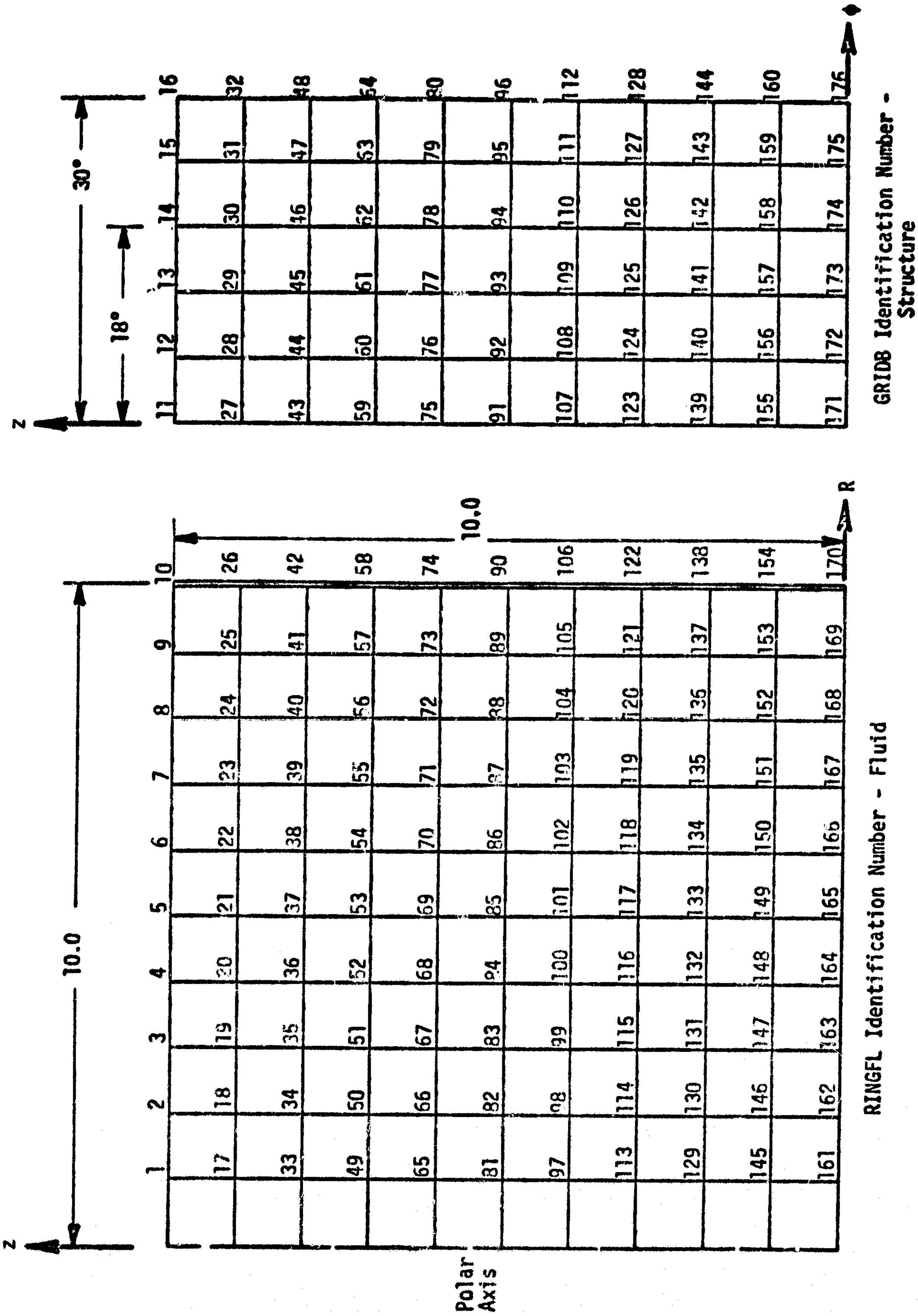

Figure 2. Elastic cylinder and gas model.

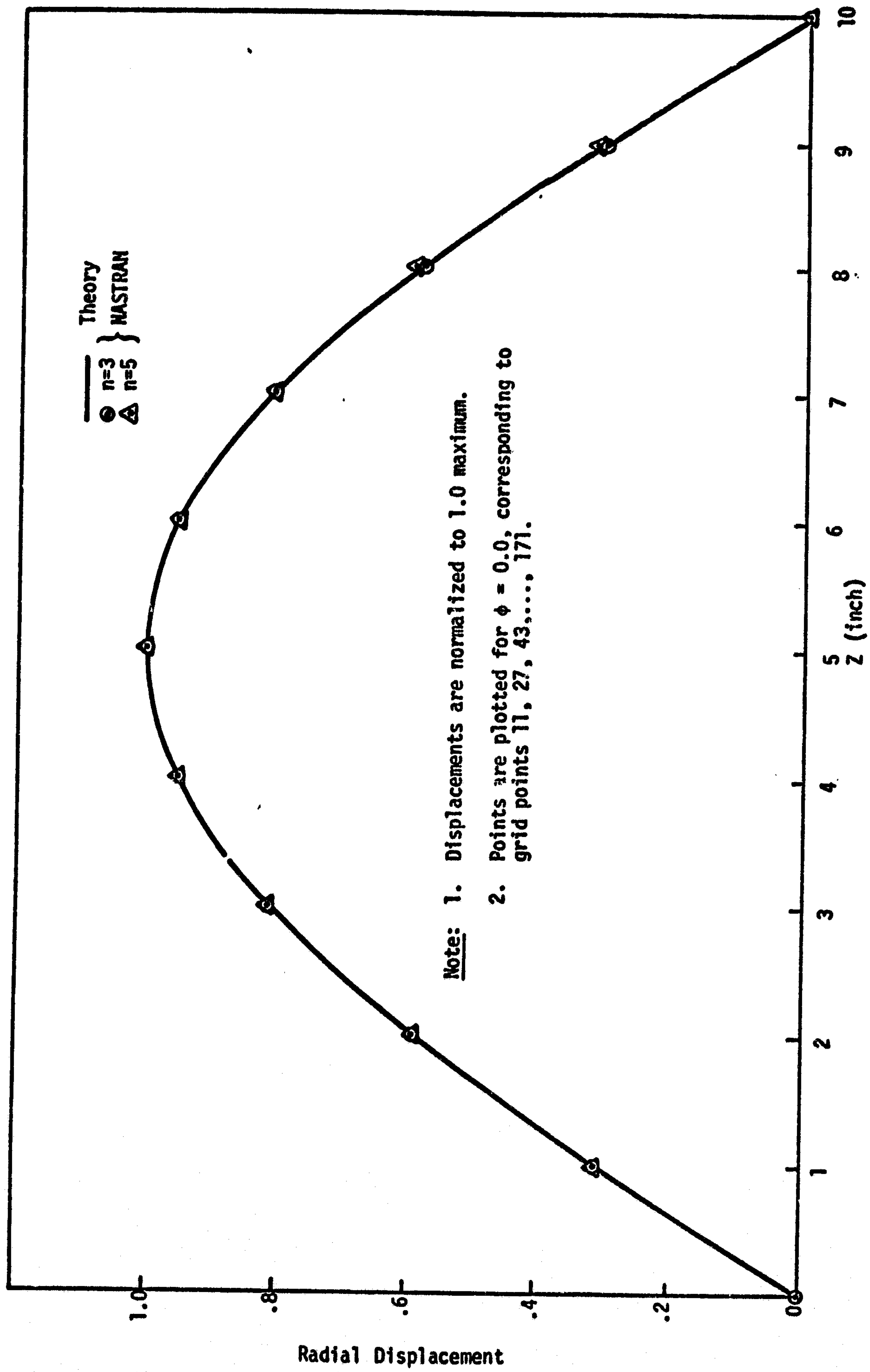

Figure 3. Radial displacement for harmonic 3 and 5 normal modes.

RIGID FORMAT No. 9, Transient Analysis - Direct Formulation

Transient Analysis of a Fluid-Filled Elastic Cylinder (9-3)

A. Description

The fluid-filled shell, used for analysis of the third harmonic, in Demonstration Problem No. 7-2 is subjected to a step change in external pressure at t = 0 of the form

$$p = p_o \sin \frac{\pi z}{\ell} \cos n\phi \quad .$$

The fluid is assumed incompressible in order to obtain an analytical solution with reasonable effort. The harmonic used is n = 3.

In addition to the cards of Demonstration Problem No. 7-2, DAREA, PRESPT, TLØAD2, and TSTEP cards are also used. Selected displacements and pressures are plotted against time.

B. Input

The finite element model is shown in Figures 1 and 2. Parameters used are:

$B = \infty$	(Bulk modulus of fluid - incompressible)
$\rho_f = 1.8 \times 10^{-2}$ lb-sec^2/in^4	(Fluid mass density)
$\rho_s = 6.0 \times 10^{-2}$ lb-sec^2/in^4	(Structure mass density)
$E = 1.6 \times 10^5$ lb/in^2	(Young's modulus for structure)
$G = 6.0 \times 10^4$ lb/in^2	(Shear modulus for structure)
$a = 10.0$ inch	(Radius of cylinder)
$\ell = 10.0$ inch	(Length of cylinder)
$h = 0.01$ inch	(Thickness of cylinder wall)
$p_o = 2.0$	(Pressure load coefficient)

C. Theory

The theory was derived with the aid of Reference 16 as in Demonstration Problem No. 7-2. Since the fluid is incompressible, it acts on the structure like a pure mass. Neglecting the bending stiffness, the equation of force on the structure is:

$$p_s = (m + m_f)\,\ddot{w} + \frac{1}{a}\frac{\partial^2 F}{\partial z^2} \quad , \tag{1}$$

where:

p_s is the loading pressure on the structure (positive outward).

$m = \rho_s h$ is the mass per area of the structure.

m_f is the apparent mass of the fluid.

w is the normal displacement (positive outward)

The function F is defined by the equation,

$$\nabla^4 F = \frac{Eh}{a}\frac{\partial^2 w}{\partial z^2} \quad . \tag{2}$$

The spatial functions of pressure, displacement, and function F may be written in the form:

$$\begin{aligned} p_s &= p_o \sin\frac{\pi z}{\ell} \cos n\phi \quad , \\ w &= w_o \sin\frac{\pi z}{\ell} \cos n\phi \quad , \\ F &= F_o \sin\frac{\pi z}{\ell} \cos n\phi \quad . \end{aligned} \tag{3}$$

where p_o, w_o, and F_o are variables with respect to time only.

Substituting Equations 3 into Equation 2 we obtain:

$$F_o = -\frac{Eh}{a}\left(\frac{\ell}{\pi}\right)^2 \frac{w_o}{\left[1 + \left(\frac{n\ell}{\pi a}\right)^2\right]^2} \quad . \tag{4}$$

Substituting Equations 3 and 4 into Equation 1 we obtain:

$$p_o = (m + m_f)\,\ddot{w}_o + \frac{Eh}{a^2\left[1 + \left(\frac{n\ell}{\pi a}\right)^2\right]^2}\,w_o \quad . \tag{5}$$

The incompressible fluid is described by the differential equation:

$$\nabla^2 p = 0 \quad . \tag{6}$$

Applying the appropriate boundary conditions to Equation 6 results in the pressure distribution:

$$p = p_r \,\text{Sin}\,\frac{\pi z}{\ell}\,\cos(n\phi)\,I_n\!\left(\frac{\pi r}{\ell}\right) \quad , \tag{7}$$

where I_n is the modified Bessel function of the first kind and p_r is an undetermined variable. The balance of pressure and flow at the boundary of the fluid, with no structural effects, is described by the equations:

$$p_o = -\,p_r\,I_n\left(\frac{\pi a}{\ell}\right) \quad , \tag{8}$$

$$\rho_f \ddot{w} = -\left.\frac{\partial p}{\partial r}\right|_{r=a} \quad . \tag{9}$$

Substituting Equations 3 and 7 into Equation 9 results in:

$$\rho_f\,\ddot{w}_o = -\frac{\pi}{\ell}\,I_n'\left(\frac{\pi a}{\ell}\right)p_r \quad . \tag{10}$$

Eliminating P_r with Equations 8 and 10 gives the expression for apparent mass, m_f:

$$p_o = I_n\left(\frac{\pi a}{\ell}\right)\frac{\rho_f \ddot{w}_o}{\frac{\pi}{\ell}\,I_n'\left(\frac{\pi a}{\ell}\right)} = m_f\,\ddot{w}_o \quad . \tag{11}$$

Substituting the expression for m_f from Equation 11 into Equation 5 results in a simple single degree of freedom system. When the applied loading pressure is a step function at $t = 0$,

$$w = \frac{p_o}{k} (1 - \cos \omega t) \sin \frac{\pi z}{\ell} \cos n\phi \quad , \tag{12}$$

where

$$\omega = \sqrt{\frac{k}{m_T}} \quad ,$$

and

$$k = \frac{Eh}{a^2\left[1 + \left(\frac{n\ell}{\pi a}\right)^2\right]^2} \quad ,$$

and

$$m_T = m + m_f = \rho_s h + \rho_f \frac{\ell}{\pi} \frac{I_n\left(\frac{\pi a}{\ell}\right)}{I_n'\left(\frac{\pi a}{\ell}\right)} \quad .$$

D. Results

A transient analysis was performed for the case n = 3 on the model and various displacements and pressures were output versus time up to one second. The theoretical frequency is calculated to be 1.580 Hertz and the period is 0.633 seconds. The displacements at two points on the structure (Point 91 is located at ϕ - 0, z = 5.0; Point 94 is located at ϕ = 18°, z = 5.0) are plotted versus time in Figure 3.

The maximum error for the first full cycle occurs at the end of the cycle. The ratio of the error to maximum displacement is 4.75%. Changes in the time step used in the transient integration algorithm did not affect the accuracy to any great extent. The most probable causes for error were the mesh size of the model and the method used to apply the distributed load. The applied load was calculated by multiplying the pressure value at the point by an associated area. The "consistent method" of assuming a cubic polynomial displacement and integrating would eliminate the extraneous response of higher modes. The method chosen in this problem, however, is typical of actual applications.

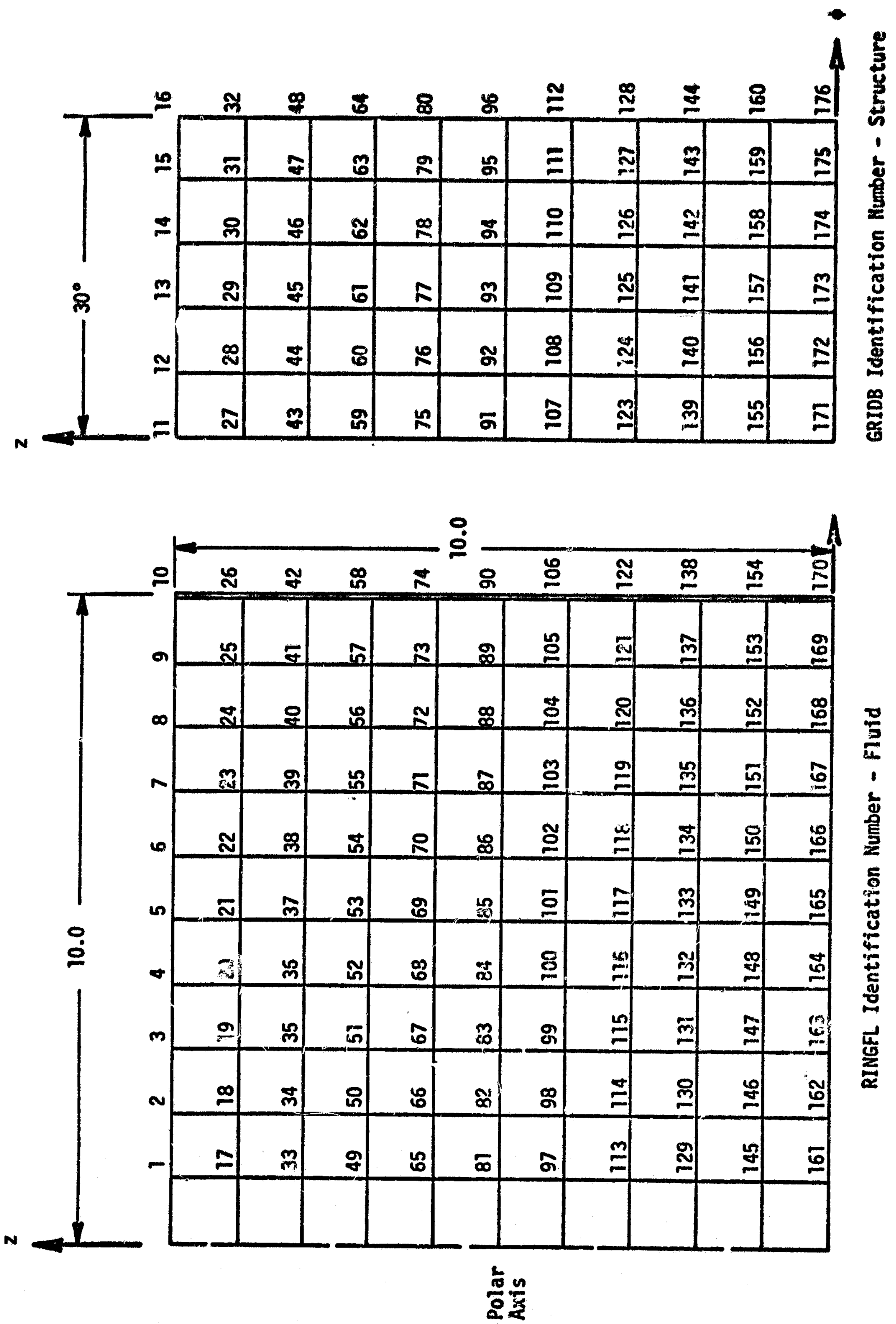

Figure 1. Transient analysis model.

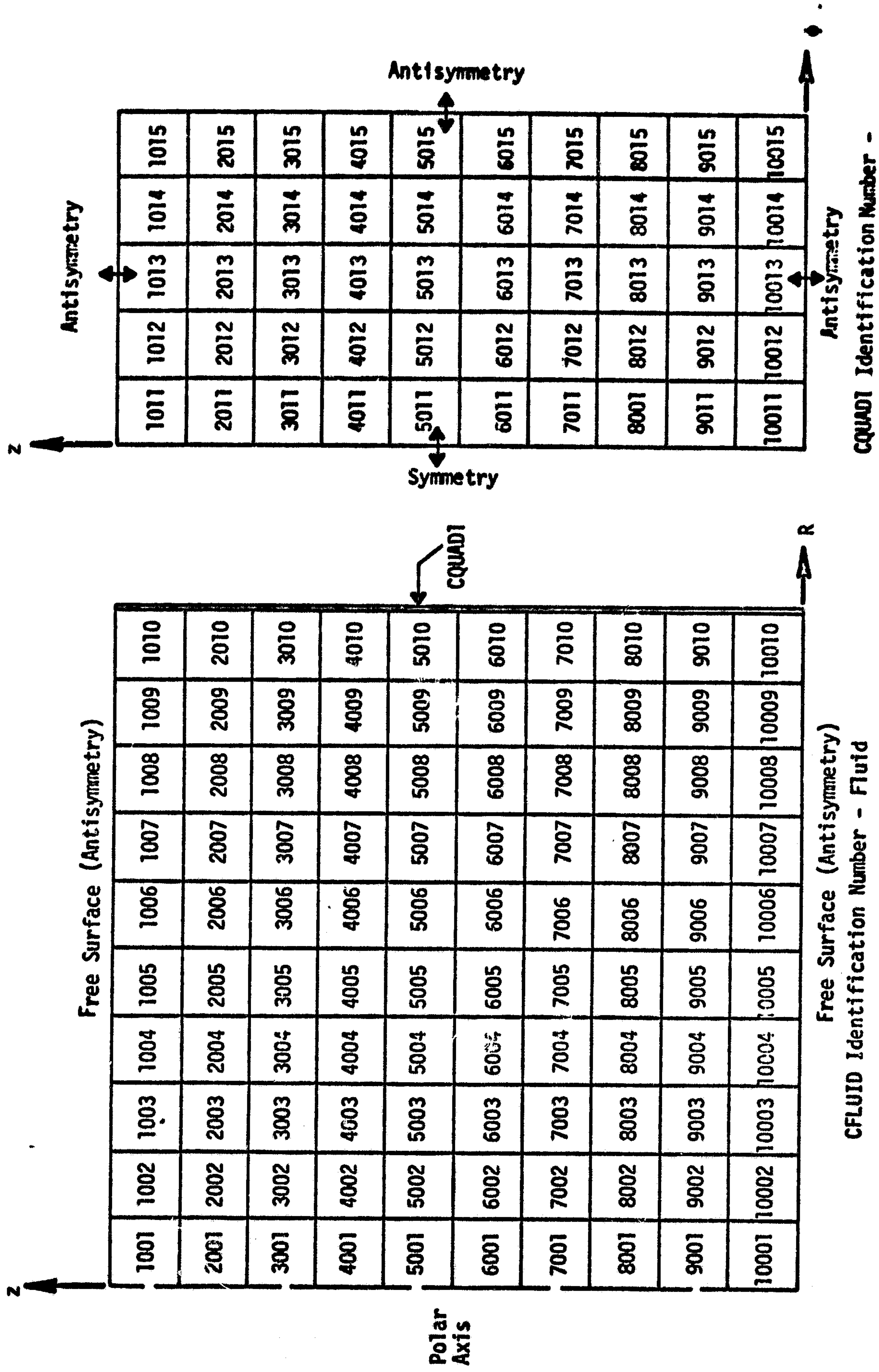

Figure 2. Transient analysis model.

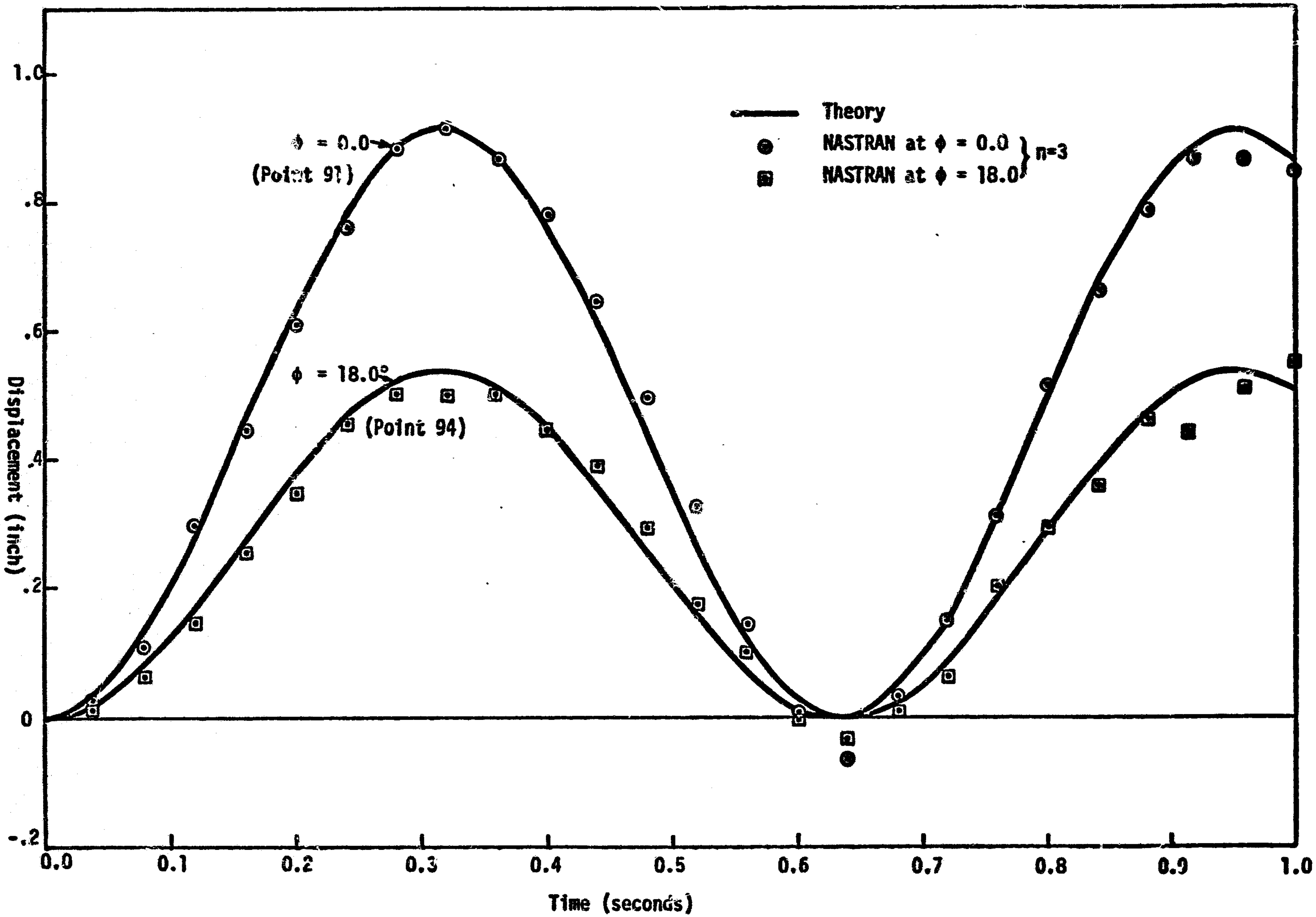

Figure 3. Displacement at midpoint (z = 5.0).

REFERENCES FOR APPENDIX

16. Berry, J. G. and Reissner, E., "The Effect of an Internal Compressible Fluid Column on the Breathing Vibrations of a Thin Pressurized Cylindrical Shell," J. of the Aeronautical Sciences, Vol. 25, No. 5, May 1958.

17. Budransky, B., "Sloshing of Liquids in Circular Canals and Spherical Tanks," J. of the Aerospace Sciences, Vol. 27, No. 3, March 1960.

18. Rayleigh, B., "The Theory of Sound," Section 330, 331, MacMillan Co., 1945.